International Journal of Mechanical Sciences 84 (2014) 120–137

Contents lists available at ScienceDirect

International Journal of Mechanical Sciences

journal homepage: www.elsevier.com/locate/ijmecsci

Three-dimensional free vibration analysis of thick cylindrical shells with general end conditions and resting on elastic foundations

Tiangui Ye, Guoyong Jin*, Shuangxia Shi, Xianglong Ma

College of Power and Energy Engineering, Harbin Engineering University, Harbin 150001, PR China

ARTICLE INFO

Article history:
Received 12 September 2013
Received in revised form
28 March 2014
Accepted 20 April 2014
Available online 26 April 2014

Keywords:
Three-dimensional
Vibration
Cylindrical shells
Arbitrary end conditions
Elastic foundations

ABSTRACT

A unified method based on the three-dimensional theory of elasticity is developed for the free vibration analysis of thick cylindrical shells with general end conditions and resting on elastic foundations. Each shell displacements, regardless of boundary conditions, is expanded as a standard Fourier cosine series supplemented with four auxiliary functions introduced to eliminate any possible discontinuities of the original displacement and its derivatives throughout the entire shell space including the boundaries and then to effectively enhance the convergence of the results. Mathematically, such series expansions are capable of representing any functions (including the exact displacement solutions). Since the displacement field is constructed adequately smooth throughout the whole solution domain, an accurate solution can obtained by using Rayleigh–Ritz procedure based on the energy functions of the shell. The current method can be universally apply to a variety of end conditions including all the classical cases and their combinations and arbitrary elastic foundations. The excellent accuracy and reliability of current solutions are demonstrated by numerical examples and comparisons with the results available in the literature. Effects of the boundary restraining parameters and foundation coefficients on frequency parameters are investigated as well. New results for thick cylindrical shells with various end conditions and resting on elastic foundations are presented, which may serve as benchmark solutions for validating new computational techniques in future.

1. Introduction

Circular cylindrical shells are one of the most important and commonly used structural elements in various kinds of military and civil applications, such as submarines, aircrafts, rockets, storage tanks and pipes. The cylindrical shells in these applications may be of recognizable thickness–length/thickness–radius ratios, subjected to general end conditions and resting on elastic foundations. They often work in complex environments which may result in violent vibration and structural collapse. Therefore, a thorough understanding of the vibration characteristics of these shells with general end conditions and resting on elastic foundations is of particular importance. Despite the many contributions to the analysis of cylindrical shells, the establishment of a unified, reliable and efficient mathematical model and approach for predicting the vibration behaviors of thick cylindrical shells with such boundary conditions remains a challenging task and is the focus of the present study.

Cylindrical shells are three-dimensional structures bounded by two, relatively close, cylindrical surfaces. The exact 3D equations of elasticity of cylindrical shells are complicated when written in curvilinear coordinates. Typically, most researchers tried to simplify such shell equations by making suitable assumptions concerning the kinematics of deformation or the state of stress through the thickness of the shells, and reduce the 3D shell problems to a variety of 2D representations with reasonable accuracy. As a result, based on different assumptions, various shell theories had been developed by pioneers. Among them, there are mainly three major theories which are usually known as: the Classical Shell Theories (CSTs), the First-order Shear Deformation Theories (FSDTs) and the Higher-order Shear Deformation Theories (HSDTs). The CSTs are based on the four simplifying assumptions of Kirchhoff–Love's hypothesis, in which transverse normal and shear deformations are neglected. Many of the previous studies regarding cylindrical shells are based on the CSTs [1–11]. However, the CSTs are limited to thin shells, for which the thickness–radius and thickness–length ratios are small. For slightly thick shells, the CSTs underestimate deflection and overestimates natural frequency due to ignoring the transverse shear deformation effect. To overcome this drawback, two-dimensional classical shell theories have been developed to take into account the effects of transverse shear deformations, which resulted in various types of FSDTs [12–15]. However, the transverse shear strains in the FSDTs are assumed to be constant through the thickness, shear correction factors have to be incorporated to adjust the transverse

* Corresponding author. Tel.: +86 451 82569458; fax: +86 451 82518264.
E-mail address: guoyongjin@hrbeu.edu.cn (G. Jin).

http://dx.doi.org/10.1016/j.ijmecsci.2014.04.017
0020-7403/

shear stiffness. To overcome the deficiency of the FSDTs and further improve the dynamic analysis of shell structures, a number of HSDTs with varying degree of refinements of the kinematics of deformation were developed [16,17]. Such modified theories are better than FSDTs for the analysis of moderately thick shells but are still inadequate for the analysis of thick shells since the transverse normal stress and strain components are ignored in the HSDTs [18]. To analyze thick shells, the three-dimensional theory of elasticity which accounts for all the transverse stress and strain components may be the best choice.

Therefore, in last decades, the three-dimensional elasticity analysis of shells has attracted the attention of several investigators. Such an analysis not only provides realistic results but also allows further insights, which cannot otherwise be predicted by CSTs, FSDTs and HSDTs analysis. Some research papers and articles oriented to such contributions may be found in following enumeration. The vibration of thick circular cylindrical shells with simply supported–simply supported (S–S) and clamped–clamped (C–C) boundary conditions on the basis of three-dimensional theory of elasticity is studied by Loy and Lam [18] using a layer wise approach. Zhou et al. [19] presented a Chebyshev–Ritz method for solving the free vibration of solid and hollow circular cylinders. A semi-analytical method was developed by Mofakhami et al. [20] to calculate the natural frequencies of finite hollow cylinders with free ends and fixed ends. A series solution of the general three-dimensional equations of linear elasticity was proposed by Hutchinson [21] to find accurate natural frequencies for the vibrations of solid elastic cylinders. Leissa and Kang [22] presented a 3D method for determining the free vibration frequencies and mode shapes of hollow bodies of revolution. A new three-dimensional refined high-order theory was presented by Khalili et al. [23] for the free vibration analysis of simply supported–simply supported and clamped–clamped homogenous isotropic circular cylindrical shells. Three-dimensional solution of the free vibration problem of homogeneous isotropic cylindrical shells and panels with a certain type of simply supported boundary condition was provided by Soldatos and Hadjigeorgiou [24] by an iterative approach. Some other contributors in this subject can be seen in Refs. [25–32]. More detailed and systematic summarizations can be seen in the excellent monographs by Leissa and Qatu [33], Qatu [34] and Soldatos [35].

This review of the existing literature clearly reveals that the information available for free vibration behavior of thick cylindrical shells is far from complete. It appears that most of the previous studies on the cylindrical shells are confined to specified classical end conditions. However, a variety of possible elastic foundation support cases such as cylindrical shells laid on or placed in a soil medium are usually encountered in practice. Moreover, the existing solution procedures are often only customized for a specific set of different end conditions, and thus typically require constant modifications of the trial functions and corresponding solution procedures to adapt to different end cases. As a result, the use of the existing solution procedures will result in very tedious calculations and be easily inundated with various classical boundaries and their combinations. Hence, it is necessary to develop a unified method which is capable of universally dealing with thick cylindrical shells subjected to general end conditions and resting on elastic foundations. Unfortunately, to the best knowledge of the authors, researches efforts on this topic are very limited. Recently, Malekzadeh et al. [36] presented a differential quadrature method for solving the free vibration of a circular cylindrical shell in contact with an elastic medium. Tj et al. [37] considered free vibrations of cylindrical shells partially buried in elastic foundations based on the finite element method. Paliwal et al. [38] studied the free vibrations of thin circular cylindrical shell on Winkler and Pasternak foundations. The wave propagation approach is employed by Shah et al. [39] and Liu et al. [40] to solve the vibrations of fluid-filled isotropic circular cylindrical shells based on elastic foundations.

In present paper, an improved Fourier series method previously proposed for the vibration analysis of beams and plates [41–44] subjected to arbitrary boundary conditions is applied to the modeling and vibration analysis of 3D cylindrical shells with general end conditions and resting on elastic foundations, aiming to provide a unified and reasonable accurate alternative to other analytical and numerical techniques. The three-dimensional elasticity theory is adopted to formulate the theoretical model. Each displacements of the cylindrical shell, regardless of boundary conditions, is expanded as a standard Fourier cosine series supplemented with four auxiliary functions introduced to ensure and accelerate the convergence of the series expansions. Since the displacement field is constructed adequately smooth throughout the whole solution domain, an accurate solution is obtained by using Rayleigh–Ritz procedure based on the energy functions of the shell. As it will become evident in what follows, the present method is capable of dealing with the vibration problems of thick cylindrical shells subjected to end conditions of arbitrary type and general elastic foundations.

2. Theoretical formulations

2.1. Description of the model and kinematic relations

As shown in Fig. 1(a), a thick circular cylindrical shell with length L, outer radius R_1, inner radius R_0 (where thickness $h=R_1-R_0$ and mean radius $R=(R_1+R_0)/2$) is considered in the present work. A cylindrical coordinate system (x, θ and r) is fixed at the shell. The x, θ and r axes are taken in the axial, circumferential and radial directions of the shell, respectively. The corresponding displacement components at any point of the shell in the axial, circumferential and radial directions are separately denoted by u, v and w. The outer surface of the shell is continuously rested on an elastic foundation represented by the Winkler/Pasternak model, in which the radial and shear stiffnesses are denoted by K_r and K_g, respectively, see Fig. 1(c). Based on the 3D shell theory, the strains during deformation for a thick circular cylindrical shell are defined as

$$\varepsilon_x=\frac{\partial u}{\partial x},\quad \varepsilon_\theta=\frac{\partial v}{r\,\partial\theta}+\frac{w}{r},\quad \varepsilon_r=\frac{\partial w}{\partial r}$$
$$\gamma_{\theta r}=\frac{\partial w}{r\,\partial\theta}+\frac{\partial v}{\partial r}-\frac{v}{r},\quad \gamma_{xr}=\frac{\partial u}{\partial r}+\frac{\partial w}{\partial x},\quad \gamma_{x\theta}=\frac{\partial u}{r\partial\theta}+\frac{\partial v}{\partial x} \tag{1}$$

where ε_x, ε_θ and ε_r are the normal strains. $\gamma_{\theta r}$, γ_{xr} and $\gamma_{x\theta}$ represent the shear strains. u, v and w denote the displacement components in the axial, circumferential and radial directions, respectively. According to the generalized Hooke's law, the corresponding stresses are defined as

$$\begin{Bmatrix}\sigma_x\\ \sigma_\theta\\ \sigma_r\\ \tau_{\theta r}\\ \tau_{xr}\\ \tau_{x\theta}\end{Bmatrix}=\begin{bmatrix}Q_{11}&Q_{12}&Q_{13}&0&0&0\\ Q_{12}&Q_{22}&Q_{23}&0&0&0\\ Q_{13}&Q_{23}&Q_{33}&0&0&0\\ 0&0&0&Q_{44}&0&0\\ 0&0&0&0&Q_{55}&0\\ 0&0&0&0&0&Q_{66}\end{bmatrix}\begin{Bmatrix}\varepsilon_x\\ \varepsilon_\theta\\ \varepsilon_r\\ \gamma_{\theta r}\\ \gamma_{xr}\\ \gamma_{x\theta}\end{Bmatrix} \tag{2}$$

where σ_x, σ_θ and σ_r are the normal stresses. $\tau_{\theta r}$, τ_{xr} and $\tau_{x\theta}$ represent the shear stressed. Q_{ij} (i, j=1–6) are the constants relating stresses with strains. For the isotropic material, they are defined as

$$Q_{11}=Q_{22}=Q_{33}=\frac{E(1-\mu)}{(1+\mu)(1-2\mu)},\quad Q_{12}=Q_{13}=Q_{23}=\frac{\mu E}{(1+\mu)(1-2\mu)},$$

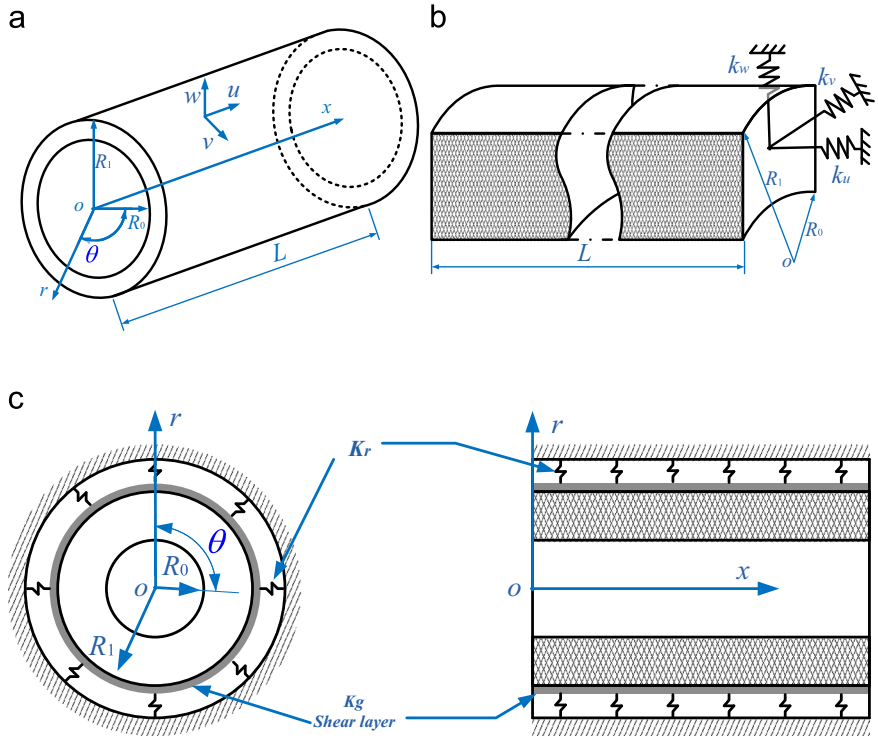

Fig. 1. Schematic diagram of a thick circular cylindrical shell: (a) the whole shell; (b) the partial cross-sectional view; (c) in contact with an elastic foundation.

$$Q_{44}=Q_{55}=Q_{66}=\frac{E}{2(1+\mu)} \tag{3}$$

where E and μ are Yong's moduli and Poisson's ratio of the material, respectively.

The boundary conditions of a thick shell can be defined as [33]

$$\sigma_{0x}-\sigma_x=0,\quad \tau_{0xr}-\tau_{xr}=0,\quad \tau_{0x\theta}-\tau_{x\theta}=0 \text{ or } u=u^0,\quad v=v^0,\quad w=w^0 \tag{4}$$

where σ_{0x}, τ_{0xr} and $\tau_{0x\theta}$ are boundary forces. u^0, v^0 and w^0 represent specified displacement functions at the boundary. Thus, at each of the shell ends, the general end conditions of the thick shell can be implemented by introducing three groups of continuously distributed linear springs (k_u, k_v and k_w) which are continuously distributed along the whole boundary area to separately simulate the boundary forces and displacements (see Fig. 1 (b)) without the need of considering of torsional spring. Specifically, k_{u0}, k_{v0} and k_{w0} denote the set of springs distributed at the edge $x=0$ and k_{uL}, k_{vL} and k_{wL} represent the other set at the end $x=L$. Therefore, all the classical homogeneous boundary conditions can be directly obtained by accordingly setting the spring constants to be extremely large or small. For instance, a clamped boundary (C) can be readily achieved by simply setting the stiffnesses of the entire boundary springs equal to infinite (which is represented by a very large number).

So far, all the needed parts of the 3D small deformation theory of elasticity are present, and they are combined to obtain the desired form of the energy expressions.

2.2. Energy expressions

In present work, the energy-oriented Rayleigh–Ritz method is employed due to the reliability of its results and efficiency in modeling and solution procedure. Thus, the first task is to define the energy expressions of the cylindrical shell. The linear elastic strain energy (U_V) of the shell is defined in integral form as:

$$U_V=\frac{1}{2}\int_0^L\int_{R_0}^{R_1}\int_0^{2\pi}\{\varepsilon_x\sigma_x+\varepsilon_\theta\sigma_\theta+\varepsilon_r\sigma_r+\gamma_{\theta r}\tau_{\theta r}+\gamma_{xr}\tau_{xr}+\gamma_{x\theta}\tau_{x\theta}\}r\,d\theta\,dr\,dx \tag{5}$$

Substituting Eqs. (1)–(3) into Eq. (5), the strain energy function of the shell can be written in terms of displacement components as

$$U_V=\frac{E}{4(1+\mu)}\int_0^L\int_{R_0}^{R_1}\int_0^{2\pi}\left\{\begin{array}{l}\frac{2\mu}{1-2\mu}\left(\frac{\partial u}{\partial x}+\frac{\partial v}{r\partial\theta}+\frac{w}{r}+\frac{\partial w}{\partial r}\right)^2+2\left(\frac{\partial u}{\partial x}\right)^2+\left(\frac{\partial w}{r\partial\theta}+\frac{\partial v}{\partial r}-\frac{v}{r}\right)^2\\+2\left(\frac{\partial w}{\partial r}\right)^2+2\left(\frac{\partial v}{r\partial\theta}+\frac{w}{r}\right)^2+\left(\frac{\partial u}{r\partial\theta}+\frac{\partial v}{\partial x}\right)^2+\left(\frac{\partial u}{\partial r}+\frac{\partial w}{\partial x}\right)^2\end{array}\right\}$$
$$r\,d\theta\,dr\,dx \tag{6}$$

The potential energy stored in the boundary springs (P_{sp}) and elastic foundation (P_{ef}) can be depicted as

$$P_{sp}=\frac{1}{2}\int_{R_0}^{R_1}\int_0^{2\pi}\left\{\begin{array}{l}[k_{u0}u^2+k_{v0}v^2+k_{w0}w^2]|_{x=0}\\+[k_{uL}u^2+k_{vL}v^2+k_{wL}w^2]|_{x=L}\end{array}\right\}r\,d\theta\,dr$$

$$P_{ef}=\frac{1}{2}\int_0^L\int_0^{2\pi}\left\{K_rw^2+K_g\left(\frac{\partial w}{\partial x}\right)^2+K_g\left(\frac{\partial w}{r\partial\theta}\right)^2\right\}\Big|_{r=R_1}R_1\,d\theta\,dx \tag{7}$$

and the kinetic energy (T) of the shell is written as

$$T=\frac{\rho}{2}\int_0^L\int_{R_0}^{R_1}\int_0^{2\pi}\left\{\left(\frac{\partial u}{\partial t}\right)^2+\left(\frac{\partial v}{\partial t}\right)^2+\left(\frac{\partial w}{\partial t}\right)^2\right\}r\,d\theta\,dr\,dx \tag{8}$$

where ρ is the density of the shell. The energy expressions are also very convenient and efficient in deriving the governing equations and boundary conditions of a structure. The energy expressions presented here are applied to obtain the equations of motion.

2.3. Equations of motion

By means of Hamilton's principle, the equations of motion of the 3D small deformation theory of elasticity of the circular

cylindrical shell in cylindrical coordinates can be written as [33]

$$L_{11}u+L_{12}v+L_{13}w=\frac{2\mu\rho}{\lambda}\frac{\partial^2 u}{\partial t^2}$$
$$L_{21}u+L_{22}v+L_{23}w=\frac{2\mu\rho}{\lambda}\frac{\partial^2 v}{\partial t^2}$$
$$L_{31}u+L_{32}v+L_{33}w=\frac{2\mu\rho}{\lambda}\frac{\partial^2 w}{\partial t^2} \tag{9}$$

where $\lambda=\mu E/(1+\mu)(1-2\mu)$, the coefficients of the linear operator L_{ij} are given below:

$$L_{11}=2(1-\mu)\left(\frac{\partial^2}{\partial r^2}+\frac{1}{r}\frac{\partial}{\partial r}-\frac{1}{r^2}\right)+(1-2\mu)\left(\frac{1}{r^2}\frac{\partial^2}{\partial\theta^2}+\frac{\partial^2}{\partial x^2}\right)$$
$$L_{12}=L_{21}=\frac{1}{r}\frac{\partial^2}{\partial r\partial\theta}-(3-4\mu)\frac{1}{r^2}\frac{\partial}{\partial\theta},\quad L_{13}=\frac{\partial^2}{\partial r\,\partial x}$$
$$L_{22}=(1-\mu)\left(\frac{\partial^2}{\partial r^2}+\frac{1}{r}\frac{\partial}{\partial r}-\frac{1}{r^2}+\frac{\partial^2}{\partial x^2}\right)+2(1-\mu)\frac{1}{r^2}\frac{\partial^2}{\partial\theta^2}$$
$$L_{23}=L_{32}=\frac{1}{r}\frac{\partial^2}{\partial\theta\partial x},\quad L_{31}=\frac{\partial^2}{\partial r\partial x}+\frac{1}{r}\frac{\partial}{\partial x}$$
$$L_{33}=(1-2\mu)\left(\frac{\partial^2}{\partial r^2}+\frac{1}{r}\frac{\partial}{\partial r}+\frac{1}{r^2}\frac{\partial^2}{\partial\theta^2}\right)+2(1-\mu)\frac{\partial^2}{\partial x^2} \tag{10}$$

It is obvious that each of the displacement components at most has second-order derivatives. The general end conditions of the thick shell are written as

$$x=0:\ k_{u0}u=\sigma_x,\ \ k_{v0}v=\tau_{x\theta},\ \ k_{w0}w=\tau_{xr}$$
$$x=a:\ k_{uL}u=-\sigma_x,\ \ k_{vL}v=-\tau_{x\theta},\ \ k_{wL}w=-\tau_{xr}$$

2.4. Admissible displacement functions and the solution procedure.

In order to guarantee convergence to the exact solutions, the constructing of appropriate admissible displacement functions is of crucial importance in the Rayleigh–Ritz procedure. For shell problems, a specially customized set of beam functions are often used as the displacement functions of the shell for each type of boundary conditions. As a result, it is inconvenient and very tedious since there are various types of end and elastic foundation conditions. A remedy to this problem is using other forms of admissible functions such as orthogonal polynomials. However, the higher order polynomials tend to become numerically unstable due to the computer round-off errors [43]. This numerical difficulty can be avoided by expressing the displacement functions in the form of a Fourier series expansion because Fourier functions constitute a complete set and exhibit an excellent numerical stability. However, when the displacements of the shell are periodically expressed as conventional Fourier series onto the entire shell space, discontinuities potentially exist in the original displacements and their derivatives at the edges except for a few simple boundary conditions. Suppose a simple linear function $f(x)=cx+d$ $(c,\ d>0)$ is defined on $[0,\ L]$. The extension of $f(x)$ onto $[-L,\ 0]$ which is even for the cosine series leads to a function that is continuous on $[-L,\ L]$ and has an identical value at $x=\pm L$. Thus, one obtains a continuous function of period $2L$, whose Fourier series will converge everywhere. However, this is not necessarily the case for a sine series which represents the odd extension of $f(x)$ onto $[-L,\ 0]$. Obviously, the new function is piecewise smooth and the corresponding Fourier series only converges to zero at $x=0$ and $x=\pm L$. In this case, the expanded expressions cannot be differentiated term-by-term, and thus the solution may not converge or converge slowly. The detailed demonstration can be found in Refs. [41,42].

To overcome this difficulty and satisfy the general boundary conditions, as well as considering the circumferential symmetry of the circular cylindrical shell, each displacements components of the circular cylindrical shell, regardless of boundary conditions, is expanded as a more robust form of modified Fourier series expansion:

$$u(x,\theta,r,t)=U(x,r)\cos(n\theta)e^{j\omega t},\quad v(x,\theta,r,t)=V(x,r)\sin(n\theta)e^{j\omega t}$$
$$w(x,\theta,r,t)=W(x,r)\cos(n\theta)e^{j\omega t} \tag{11}$$

where non-negative integer n represents the circumferential wave number of the corresponding mode. Distinctly, $n=0$ means axisymmetric vibration. Rotating the symmetry axes by $\pi/2$, another set of free vibration modes can be obtained, which corresponds to an interchange of cos $(n\theta)$ and sin $(n\theta)$ in Eq. (11) and $n=0$ representing torsional vibration in such a case [19]. ω denotes the eigenfrequency of the cylindrical shell and $j=\sqrt{-1}$. $U(x,\ r)$, $V(x,\ r)$ and $W(x,\ r)$ are the robust form of modified Fourier series expansions, they are defined as [44]

$$U(x,r)=\sum_{m=0}^{\infty}\sum_{q=0}^{\infty}A_{mq}\cos\lambda_m x\cos\lambda_q r+\sum_{m=0}^{\infty}\sum_{l=1}^{2}A^r_{lm}\zeta_l(r)\cos\lambda_m x+\sum_{l=1}^{2}\sum_{q=0}^{\infty}A^x_{lq}\zeta_l(x)\cos\lambda_q r$$
$$V(x,r)=\sum_{m=0}^{\infty}\sum_{q=0}^{\infty}B_{mq}\cos\lambda_m x\cos\lambda_q r+\sum_{m=0}^{\infty}\sum_{l=1}^{2}B^r_{lm}\zeta_l(r)\cos\lambda_m x+\sum_{l=1}^{2}\sum_{q=0}^{\infty}B^x_{lq}\zeta_l(x)\cos\lambda_q r$$
$$W(x,r)=\sum_{m=0}^{\infty}\sum_{q=0}^{\infty}C_{mq}\cos\lambda_m x\cos\lambda_q r+\sum_{m=0}^{\infty}\sum_{l=1}^{2}C^r_{lm}\zeta_l(r)\cos\lambda_m x+\sum_{l=1}^{2}\sum_{q=0}^{\infty}C^x_{lq}\zeta_l(x)\cos\lambda_q r \tag{12}$$

where $\lambda_m=m\pi/L$ and $\lambda_q=q\pi/h$. A_{mq}, B_{mq} and C_{mq} denote the Fourier expanded coefficients for the displacement components in the x, θ and r directions, respectively. $A^r_{lm}, A^x_{lq}, B^r_{lm}, B^x_{lq}$ and C^r_{lm}, C^x_{lq} are the corresponding supplemented coefficients. All of them need to be determined in future. $\zeta_l(r)$, $l=1, 2$ represent a set of supplementary functions defined over $[0,\ h]$ to take care of any possible discontinuities of the original displacements and their derivatives throughout the whole shell including the boundaries and then to effectively enhance the convergence of the results. Similarly,$\zeta_l(x)$ $l=1,\ 2$ are the other set of auxiliary terms respect to variable x. According to Eq. (10), each of the displacements components at most has second-order derivatives, thus, it is required that at least second-order derivatives of these admissible functions exist and are continuous at any point on the shell. Such requirements can be readily satisfied by choosing simple polynomials as follows:

$$\zeta_1(x)=x\left(\frac{x}{L}-1\right)^2,\quad \zeta_2(x)=\frac{x^2}{L}\left(\frac{x}{L}-1\right),\quad \zeta_1(r)=r\left(\frac{r}{h}-1\right)^2,$$
$$\zeta_2(r)=\frac{r^2}{h}\left(\frac{r}{h}-1\right) \tag{13}$$

It is easy to verify that

$$\zeta_1(0)=\zeta_1(L)=\zeta_1'(L)=0,\quad \zeta_1'(0)=1$$
$$\zeta_2(0)=\zeta_2(L)=\zeta_2'(0)=0,\quad \zeta_2'(L)=1 \tag{14}$$

Similar conditions exist for the r-related polynomials, $\zeta_l(r)$. It can be proven mathematically that the modified Fourier series given in Eq. (12) can be simply differentiated, through term-by-term, to obtain uniformly convergent series expansions for up to the second-order derivatives. Also, the series expansions given in Eq. (12) are able to expand and uniformly converge to any function including the actual displacements. More information about the modified Fourier series can be seen in Refs. [14,15,41–44]. Since the series expression has to be truncated numerically, the proposed solution should be understood as a solution with arbitrary precision. In actual calculations, we truncate the infinite series expression to M and Q to obtain the results with acceptable accuracy.

It should be remarked here that the modified Fourier series expressions given in Eq. (12) are complete series defined on the interval of $[0, L] \otimes [0, h]$. Thus, a coordinate transformation from r (for $r \in [R_0, R_1]$, to $\bar{r} \in [0, h]$) needs to be introduced to implement the present analysis. Therefore, the robust form of modified Fourier series expansions given in Eq. (12) is rewritten as

$$U(x,\bar{r}) = \sum_{m=0}^{\infty}\sum_{q=0}^{\infty} A_{mq} \cos \lambda_m x \cos \lambda_q \bar{r} + \sum_{m=0}^{\infty}\sum_{l=1}^{2} A^r_{lm}\zeta_l(\bar{r}) \cos \lambda_m x + \sum_{l=1}^{2}\sum_{q=0}^{\infty} A^x_{\ln}\zeta_l(x) \cos \lambda_q \bar{r}$$

$$V(x,\bar{r}) = \sum_{m=0}^{\infty}\sum_{q=0}^{\infty} B_{mq} \cos \lambda_m x \cos \lambda_q \bar{r} + \sum_{m=0}^{\infty}\sum_{l=1}^{2} B^r_{lm}\zeta_l(\bar{r}) \cos \lambda_m x + \sum_{l=1}^{2}\sum_{q=0}^{\infty} B^x_{\ln}\zeta_l(x) \cos \lambda_q \bar{r}$$

$$W(x,\bar{r}) = \sum_{m=0}^{\infty}\sum_{q=0}^{\infty} C_{mq} \cos \lambda_m x \cos \lambda_q \bar{r} + \sum_{m=0}^{\infty}\sum_{l=1}^{2} C^r_{lm}\zeta_l(\bar{r}) \cos \lambda_m x + \sum_{l=1}^{2}\sum_{q=0}^{\infty} C^x_{\ln}\zeta_l(x) \cos \lambda_q \bar{r} \quad (15)$$

thus, the energy expressions of the shell are rewritten as

$$U_V = \frac{E}{4(1+\mu)}\int_0^L\int_0^h\int_0^{2\pi} \left\{ \begin{array}{l} \frac{2\mu}{1-2\mu}\left(\frac{\partial u}{\partial x}+\frac{\partial v}{(\bar{r}+R_0)\partial\theta}+\frac{w}{(\bar{r}+R_0)}+\frac{\partial w}{\partial \bar{r}}\right)^2 \\ +2\left(\frac{\partial u}{\partial x}\right)^2+2\left(\frac{\partial v}{(\bar{r}+R_0)\partial\theta}+\frac{w}{(\bar{r}+R_0)}\right)^2 \\ +\left(\frac{\partial u}{(\bar{r}+R_0)\partial\theta}+\frac{\partial v}{\partial x}\right)^2+\left(\frac{\partial u}{\partial \bar{r}}+\frac{\partial w}{\partial x}\right)^2 \\ +2\left(\frac{\partial w}{\partial \bar{r}}\right)^2+\left(\frac{\partial w}{(\bar{r}+R_0)\partial\theta}+\frac{\partial v}{\partial \bar{r}}-\frac{v}{(\bar{r}+R_0)}\right)^2 \end{array} \right\} (\bar{r}+R_0)d\theta\, d\bar{r}\, dx \quad (16)$$

$$P_{sp} = \frac{1}{2}\int_0^h\int_0^{2\pi} \left\{ \begin{array}{l} [k_{u0}u^2+k_{v0}v^2+k_{w0}w^2]|_{x=0} \\ +[k_{uL}u^2+k_{vL}v^2+k_{wL}w^2]|_{x=L} \end{array} \right\} (\bar{r}+R_0)d\theta\, d\bar{r}$$

$$P_{ef} = \frac{1}{2}\int_0^L\int_0^{2\pi} \left\{ K_r w^2 + K_g\left(\frac{\partial w}{\partial x}\right)^2 + K_g\left(\frac{\partial w}{(\bar{r}+R_0)\partial\theta}\right)^2 \right\}|_{\bar{r}=h} R_1\, d\theta\, dx \quad (17)$$

$$T = \frac{\rho}{2}\int_0^L\int_0^h\int_0^{2\pi} \left\{ \left(\frac{\partial u}{\partial t}\right)^2+\left(\frac{\partial v}{\partial t}\right)^2+\left(\frac{\partial w}{\partial t}\right)^2 \right\} (\bar{r}+R_0)d\theta\, d\bar{r}\, dx \quad (18)$$

Once the admissible displacement functions and energy functions of the shell are established, the following task is to determine

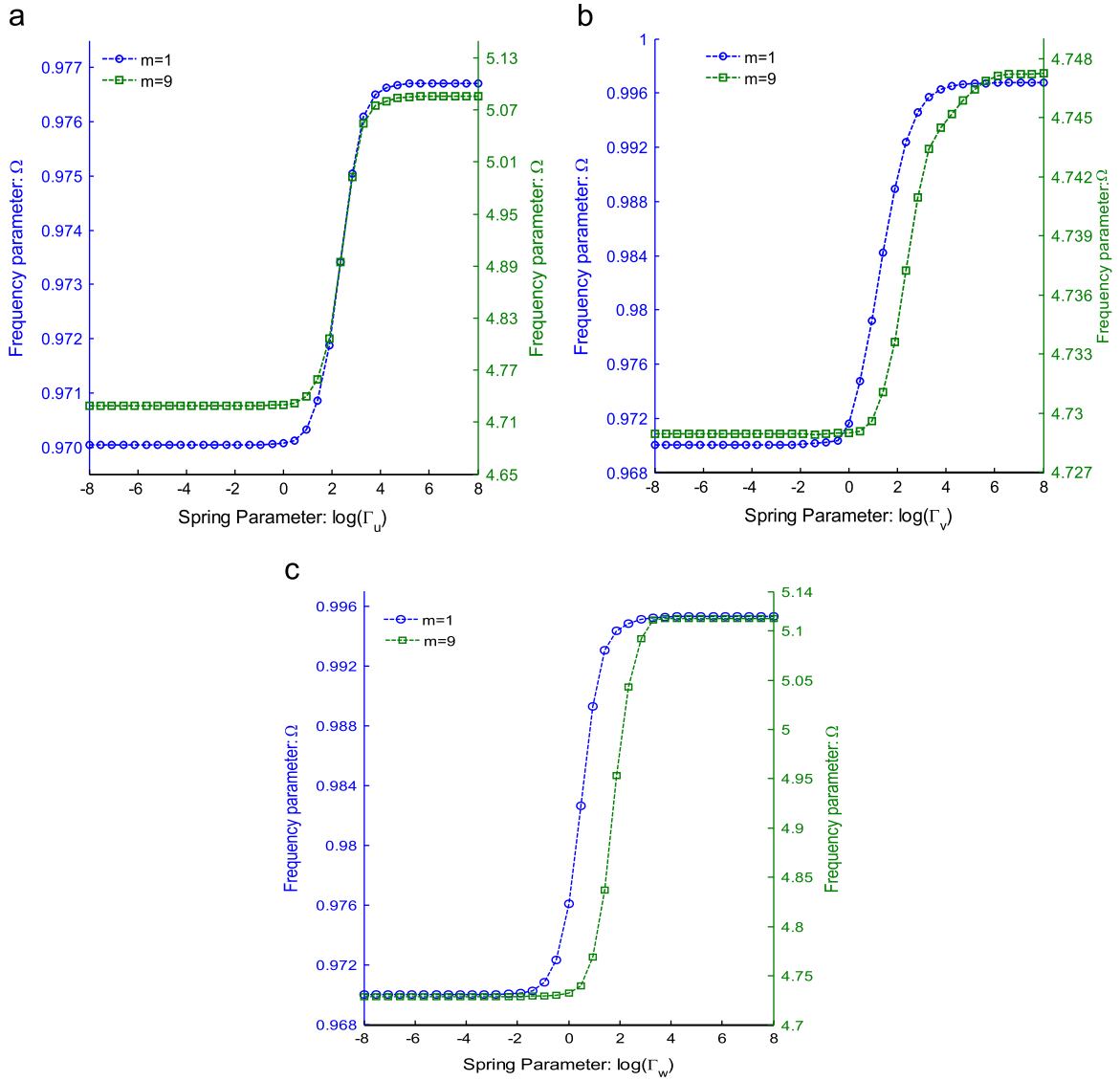

Fig. 2. The effect of boundary spring stiffnesses on frequency parameters $\Omega = \omega R_1\sqrt{\rho/G}$ for a thick cylindrical shell: (a) Γ_u; (b) Γ_v; (c) Γ_w.

the coefficients in the admissible functions. The Lagrangian energy function (L) of the shell can be expressed in terms of strain energy, kinetic energy and potential energy stored in boundary springs and foundation of the shell system as

$$L = T - U_V - P_{sp} - P_{ef} \tag{19}$$

Substituting Eqs. (16)–(18) into Eq. (19) and minimizing the total expression of the Lagrangian energy function with respect to the undetermined coefficients:

$$\frac{\partial L}{\partial \alpha} = 0 \quad \alpha = A_{mq}, A^r_{lm}, A^x_{lq}, B_{mq}, B^r_{lm}, B^x_{lq}, C_{mq}, C^r_{lm}, C^x_{lq} \tag{20}$$

a total of $3*\{(M+1)*(Q+1)+2*(M+Q+2)\}$ equations related to corresponding coefficients can be achieved and summed up in matrix form as

$$(\mathbf{K} - \omega^2 \mathbf{M})\mathbf{G} = \mathbf{0} \tag{21}$$

in which $\mathbf{K}$ is the stiffness matrix for the structure, $\mathbf{M}$ is the mass matrix. Both of them are symmetric matrixes and they can be expressed as

$$\mathbf{K} = \begin{bmatrix} \mathbf{K}_{1,1} & \mathbf{K}_{1,2} & \mathbf{K}_{1,3} & \cdots & \mathbf{K}_{1,9} \\ \mathbf{K}^T_{1,2} & \mathbf{K}_{2,2} & \mathbf{K}_{2,3} & \cdots & \mathbf{K}_{2,9} \\ \mathbf{K}^T_{1,3} & \mathbf{K}^T_{2,3} & \mathbf{K}_{3,3} & \cdots & \mathbf{K}_{3,9} \\ \vdots & \vdots & \vdots & \ddots & \vdots \\ \mathbf{K}^T_{1,9} & \mathbf{K}^T_{2,9} & \mathbf{K}^T_{3,9} & \cdots & \mathbf{K}_{9,9} \end{bmatrix},$$

$$\mathbf{M} = \begin{bmatrix} \mathbf{M}_{1,1} & \mathbf{M}_{1,2} & \mathbf{M}_{1,3} & \cdots & \mathbf{M}_{1,9} \\ \mathbf{M}^T_{1,2} & \mathbf{M}_{2,2} & \mathbf{M}_{2,3} & \cdots & \mathbf{M}_{2,9} \\ \mathbf{M}^T_{1,3} & \mathbf{M}^T_{2,3} & \mathbf{M}_{3,3} & \cdots & \mathbf{M}_{3,9} \\ \vdots & \vdots & \vdots & \ddots & \vdots \\ \mathbf{M}^T_{1,9} & \mathbf{M}^T_{2,9} & \mathbf{M}^T_{3,9} & \cdots & \mathbf{M}_{9,9} \end{bmatrix} \tag{22}$$

The elements of the sub-matrices $\mathbf{K}_{i,j}$ and $\mathbf{M}_{i,j}$ (i, j=1–9) are given in Appendix A. $\mathbf{G}$ is the vector of unknown coefficients, is written as

$$G = [\mathbf{G}^u, \mathbf{G}^v, \mathbf{G}^w]^T \tag{23}$$

Table 1
Convergence of the first ten longitudinal modal frequency parameters $\Omega = \omega R_1\sqrt{p/G}$ for an F–F circular cylindrical shell (R_0/R_1=0.5, L/R_1=2, μ=0.3, K_r=0 and K_g=0).

n	$M \times Q$	Modes									
		m=1	m=2	m=3	m=4	m=5	m=6	m=7	m=8	m=9	m=10
1	5 × 5	1.6042	1.8934	2.4808	2.9315	3.0795	3.2392	4.0290	4.5311	4.6752	5.6873
	6 × 6	1.6041	1.8933	2.4808	2.9312	3.0795	3.2385	4.0286	4.5239	4.6749	5.6623
	7 × 7	1.6041	1.8932	2.4807	2.9312	3.0795	3.2383	4.0285	4.5233	4.6749	5.6607
	8 × 8	1.6041	1.8932	2.4807	2.9311	3.0794	3.2382	4.0284	4.5228	4.6748	5.6600
	9 × 9	1.6041	1.8932	2.4807	2.9311	3.0794	3.2381	4.0284	4.5227	4.6748	5.6598
	10 × 10	1.6041	1.8932	2.4807	2.9311	3.0794	3.2381	4.0284	4.5226	4.6748	5.6597
	11 × 11	1.6041	1.8932	2.4807	2.9311	3.0794	3.2381	4.0284	4.5226	4.6748	5.6597
	Ref. [19]	1.6041	1.8932	2.4807	2.9311	3.0794	3.2380	4.0284	4.5225	4.6748	5.6596
2	5 × 5	0.9702	1.0455	1.9355	2.4982	3.2934	3.4423	4.2660	4.3189	4.7376	5.1825
	6 × 6	0.9701	1.0452	1.9354	2.4981	3.2932	3.4408	4.2656	4.3188	4.7304	5.1814
	7 × 7	0.9701	1.0452	1.9352	2.4981	3.2930	3.4406	4.2655	4.3187	4.7294	5.1814
	8 × 8	0.9700	1.0452	1.9352	2.4981	3.2930	3.4403	4.2654	4.3187	4.7289	5.1813
	9 × 9	0.9700	1.0451	1.9351	2.4981	3.2930	3.4403	4.2654	4.3187	4.7287	5.1813
	10 × 10	0.9700	1.0451	1.9351	2.4981	3.2930	3.4402	4.2654	4.3187	4.7286	5.1812
	11 × 11	0.9700	1.0451	1.9351	2.4981	3.2929	3.4401	4.2654	4.3187	4.7286	5.1812
	Ref. [19]	0.9700	1.0451	1.9351	2.4981	3.2929	3.4401	4.2654	4.3187	4.7258	5.1812

Table 2
Convergence and comparison of the first nine frequency parameters $\Omega = 2\omega R_1\sqrt{p/E}$ for an F–F solid cylinder (L/R_1=4, μ=0.3, K_r=0 and K_g=0).

Method	M	N	Mode number								
			1	2	3	4	5	6	7	8	9
Liew and Hung [32]	5	5	0.9594	0.9594	0.9742	1.5467	1.7751	1.7751	1.9483	2.5938	2.5938
	6	5	0.9594	0.9594	0.9742	1.5467	1.7751	1.7751	1.9483	2.5938	2.5938
	5	6	0.9594	0.9594	0.9742	1.5467	1.7751	1.7751	1.9483	2.5938	2.5938
	5	7	0.9594	0.9594	0.9742	1.5467	1.7751	1.7751	1.9483	2.5938	2.5938
	5	8	0.9594	0.9594	0.9742	1.5467	1.7751	1.7751	1.9483	2.5938	2.5938
Present	5	5	0.9597	0.9597	0.9742	1.5467	1.7767	1.7767	1.9483	2.5979	2.5979
	6	5	0.9595	0.9595	0.9742	1.5467	1.7755	1.7755	1.9483	2.5964	2.5964
	5	6	0.9597	0.9597	0.9742	1.5467	1.7767	1.7767	1.9483	2.5977	2.5977
	5	7	0.9597	0.9597	0.9742	1.5467	1.7767	1.7767	1.9483	2.5976	2.5976
	5	8	0.9597	0.9597	0.9742	1.5467	1.7767	1.7767	1.9483	2.5976	2.5976
	6	8	0.9595	0.9595	0.9742	1.5467	1.7755	1.7755	1.9483	2.5963	2.5963
	7	8	0.9595	0.9595	0.9742	1.5467	1.7753	1.7753	1.9483	2.5943	2.5943
	8	8	0.9595	0.9595	0.9742	1.5467	1.7752	1.7752	1.9483	2.5941	2.5941
	9	8	0.9595	0.9595	0.9742	1.5467	1.7751	1.7751	1.9483	2.5939	2.5939
	10	8	0.9595	0.9595	0.9742	1.5467	1.7751	1.7751	1.9483	2.5938	2.5938
	11	8	0.9595	0.9595	0.9742	1.5467	1.7751	1.7751	1.9483	2.5938	2.5938
	11	9	0.9595	0.9595	0.9742	1.5467	1.7751	1.7751	1.9483	2.5938	2.5938

where

$$\mathbf{G}^u = [A_{00}, \ldots, A_{mq}, \ldots, A_{MQ}, A^r_{10}, \ldots, A^r_{lm}, \ldots, A^r_{2M}, A^x_{10}, \ldots, A^x_{lq}, \ldots, A^x_{2Q}]$$

$$\mathbf{G}^v = [B_{00}, \ldots, B_{mq}, \ldots, B_{MQ}, B^r_{10}, \ldots, B^r_{lm}, \ldots, B^r_{2M}, B^x_{10}, \ldots, B^x_{lq}, \ldots, B^x_{2Q}]$$

$$\mathbf{G}^w = [C_{00}, \ldots, C_{mq}, \ldots, C_{MQ}, C^r_{10}, \ldots, C^r_{lm}, \ldots, C^r_{2M}, C^x_{10}, \ldots, C^x_{lq}, \ldots, C^x_{2Q}]$$

The frequencies and modes of the shell can be determined easily by solving the standard characteristic equation. Once the eigenvector **G** is determined for a given frequency, the mode shapes of the shell can be determined by substituting the coefficients **G** into the admissible functions. Even though this study is focused on the free vibration of a thick cylindrical shell with general end conditions and resting on elastic foundations, the forced vibration can be readily predicted by adding the work done by external force in Eq. (19) and summing the loading vector **F** of external force on the right side of Eq. (21). Thus, the characteristic equation for the forced vibration of the shell is readily obtained.

3. Numerical examples and discussion

With the theoretical formulations described in previous sections, several vibration results for thick cylindrical shells subjected to general end conditions and resting on elastic foundations are presented in this section to illustrate the capacity and reliability of the current solution. Summarizing, the discussion is arranged as follows: First of all, end conditions of the shells are defined in terms of boundary spring parameters. The convergence and efficiency of the present method is studied and the model is checked by comparing with results in the open literature. Then, cylindrical shells with various classical end conditions and their combinations are studied, and some selected modal shapes are depicted. Influence of the geometry parameters are discussed as well. Finally, numerical results for cylindrical shells resting on elastic foundations are presented and effects of the foundation coefficients are investigated.

Table 3
Computational time (second) versus number of modes for a thick shell with various boundary conditions ($R_0/R_1=0.5$, $L/R_1=2$, $\mu=0.3$, $K_r=0$ and $K_g=0$, $M^*Q=11^*11$).

Boundary conditions	Number of modes										
	$n=0$				$n=1$				$n=2$		
	10	20	40		10	20	40		10	20	40
F–F	0.998	0.967	1.062	0.831	1.066	1.170	1.374	0.831	1.101	1.176	1.395
F–S	0.980	0.967	1.029	0.831	1.117	1.183	1.423	0.831	1.114	1.178	1.393
F–C	0.991	0.969	1.046	0.831	1.093	1.188	1.395	0.831	1.099	1.179	1.400
S–S	0.978	1.000	1.237	0.831	1.105	1.194	1.376	0.831	1.093	1.222	1.401
S–C	0.982	0.961	1.076	0.831	1.115	1.183	1.402	0.831	1.105	1.212	1.406
C–C	0.986	0.964	1.039	0.831	1.190	1.189	1.401	0.831	1.086	1.185	1.415

Table 4
Comparison of frequency parameters $\Omega=\omega h/\pi\sqrt{p/G}$ for an S–S circular cylindrical shell ($h/R=0.1$, $\mu=0.3$, $K_r=0$, $K_g=0$, $m=1$).

L/R	Present			Ref. [31]			Ref. [23]		
	$n=1$	$n=2$	$n=3$	$n=1$	$n=2$	$n=3$	$n=1$	$n=2$	$n=3$
2	0.03099	0.01906	0.01814	0.03100	0.01907	0.01814	0.03100	0.01906	0.01813
1	0.04781	0.03971	0.03642	0.04784	0.03927	0.03643	0.04779	0.03969	0.03641
0.5	0.07616	0.07681	0.07931	0.07618	0.07684	0.07935	0.07607	0.07675	0.07927
0.25	0.20527	0.20801	0.21259	0.20529	0.20802	0.21261	0.20525	0.20800	0.21260

Table 5
Comparison of frequency parameters $\Omega=\omega L\sqrt{p(1+\mu)/E}$ for a thick cylindrical shell subjected to F–F, C–F and C–C end conditions ($h/R=0.3$, $\mu=0.3$, $L/R=1$, $K_r=0$, $K_g=0$).

Boundary conditions	n	LW-DQ [36]			FEM [36]			Present		
		$m=1$	$m=2$	$m=3$	$m=1$	$m=2$	$m=3$	$m=1$	$m=2$	$m=3$
F–F	1	0.0000	0.0001	1.0710	0.0000	0.0001	1.0734	0.0000	0.0001	1.0709
	2	0.2576	0.3800	1.3533	0.2608	0.3831	1.3594	0.2576	0.3799	1.3532
	3	0.6884	0.9253	1.8689	0.6890	0.9377	1.8794	0.6884	0.9252	1.8689
	4	1.2302	1.5160	2.4754	1.2525	1.5307	2.4917	1.2302	1.5158	2.4753
	5	1.8427	2.1343	3.1169	1.8694	2.1532	3.1417	1.8426	2.1341	3.1169
C–F	1	0.7514	1.7563	1.8800	0.7546	1.7692	1.8996	0.7516	1.7569	1.8811
	2	0.6620	1.8962	2.1305	0.6713	1.9256	2.1557	0.6622	1.8982	2.1325
	3	0.9246	2.0610	2.5165	0.9301	2.0668	2.5482	0.9247	2.0632	2.5179
	4	1.4021	2.4030	2.9919	1.4282	2.4646	3.0342	1.4021	2.4052	2.9930
	5	1.9814	2.8666	3.5251	2.0228	2.8571	3.5628	1.9814	2.8687	3.5259
C–C	1	1.7860	2.6043	3.4148	1.7972	2.6222	3.4192	1.7911	2.6049	3.4259
	2	1.7452	3.2942	3.4921	1.7573	3.3114	3.5150	1.7507	3.2948	3.5027
	3	1.8867	3.6024	3.9416	1.8862	3.6320	3.9257	1.8921	3.6111	3.9443
	4	2.1966	3.8126	4.2757	2.2072	3.8228	4.3215	2.2012	3.8204	4.2781
	5	2.6385	4.1302	4.7010	2.6617	4.1327	4.7322	2.6421	4.1375	4.7028

3.1. Boundary springs study

In the present work, the general end conditions of the shell are implemented by introducing three groups of continuously distributed linear springs at each of the shell ends to separately simulate the boundary forces and displacements. Therefore, arbitrary end conditions of the shell can be easily generated by assigning the boundary springs at proper stiffnesses. For instance, a clamped end (C) can be readily achieved by simply setting the stiffnesses of the entire springs equal to infinitely large. However, the 'infinite large' is represented by a sufficiently large number in actual calculations. Thus, effects of the restraint stiffness of boundary spring on the modal characteristics should be investigated. In the first example, effects of restraint stiffness of boundary springs on a cylindrical

Table 6
Frequency parameters $\Omega=\omega R_1\sqrt{p/G}$ for a circular cylindrical shell subjected to various end conditions ($L/R_1=3$, $R_0/R_1=0.5$, $\mu=0.3$, $K_r=0$, $K_g=0$).

Boundary conditions	n	Modes								
		$m=1$	$m=2$	$m=3$	$m=4$	$m=5$	$m=6$	$m=7$	$m=8$	$m=9$
F–F	0	1.6004	2.1554	2.1824	2.3634	2.4640	2.9471	3.6445	3.7409	4.6300
	1	1.1605	1.3969	2.0519	2.1411	2.7433	2.8606	2.9513	3.3761	3.3975
	2	0.9745	1.0160	1.3782	2.0346	2.7227	2.7289	3.2773	3.5929	4.0668
	3	2.2928	2.3236	2.5134	2.9240	3.5036	3.8369	4.2102	4.4111	4.8382
F–S	0	1.6004	2.1630	2.2865	2.4630	2.7998	3.5527	3.6478	4.4368	5.2854
	1	0.8407	1.3974	1.7937	2.0657	2.6428	2.7789	3.0641	3.3440	3.5538
	2	0.9889	1.2314	1.8777	2.5713	2.8086	3.0404	3.5970	3.7922	4.2595
	3	2.3045	2.4502	2.8260	3.4140	3.9055	4.0707	4.3806	4.6416	5.1475
S–S	0	1.6004	2.2215	2.4587	2.6689	3.3739	3.6468	4.2406	5.1896	5.2857
	1	0.6230	1.3545	1.5142	2.0230	2.3879	2.8197	3.2155	3.2905	3.6036
	2	1.1208	1.6925	2.5267	2.6809	2.9997	3.4561	3.6297	4.3475	4.4260
	3	2.3985	2.7268	3.3167	3.9573	4.0832	4.1504	4.6197	4.9488	5.2312
F–C	0	0.8508	2.1155	2.2028	2.4608	2.7831	3.0055	3.6589	4.4440	4.5517
	1	0.2675	0.8744	1.6232	1.9137	2.5237	2.7223	3.0192	3.1060	3.5883
	2	1.0012	1.2890	1.9536	2.6002	2.9913	3.3269	3.8248	4.0545	4.3593
	3	2.3070	2.4767	2.8737	3.4481	3.9510	4.2442	4.5540	4.9430	5.3157
C–C	0	1.6949	2.3123	2.5607	2.8814	3.5910	3.6508	4.4199	5.2192	5.4114
	1	0.8157	1.6113	2.1297	2.5317	2.8945	3.3635	3.4640	3.4778	4.3041
	2	1.2399	1.8299	2.6428	3.0643	3.5672	3.7992	4.4677	4.5159	4.5571
	3	2.4455	2.8198	3.4086	4.1014	4.2571	4.7295	5.0429	5.4104	5.9361

Table 7
Frequency parameters $\Omega=\omega R_1\sqrt{p/G}$ for a solid cylinder subjected to various boundary conditions ($L/R_1=3$, $\mu=0.3$, $K_r=0$, $K_g=0$).

Boundary conditions	n	Modes								
		$m=1$	$m=2$	$m=3$	$m=4$	$m=5$	$m=6$	$m=7$	$m=8$	$m=9$
F–F	0	1.6387	2.8098	2.9218	2.9928	3.5003	4.0263	4.0421	4.1601	4.8144
	1	1.1761	1.7735	2.5332	2.5900	2.8882	2.9565	3.3410	3.6864	3.7323
	2	2.1066	2.1627	2.3501	2.6928	3.3610	3.4066	4.0727	4.0794	4.3616
	3	3.2451	3.2594	3.6176	3.7343	4.2021	4.4099	4.8891	4.9062	5.5103
F–S	0	1.6387	2.8112	2.9542	3.4978	3.6679	4.0295	4.1602	4.4405	4.8308
	1	0.8735	1.7670	2.1002	2.5561	2.8788	3.0596	3.3121	3.5565	3.9529
	2	2.1346	2.3341	2.6802	3.1462	3.3670	3.7409	4.0972	4.4184	4.5041
	3	3.2521	3.6041	3.7479	4.1805	4.2956	4.6405	4.8963	5.2209	5.5705
S–S	0	1.6388	2.8131	3.4860	3.5620	3.8317	4.1378	4.2160	4.7026	5.0439
	1	0.6359	1.6857	1.8412	2.4635	2.7540	3.0906	3.2352	3.8011	3.9642
	2	2.3265	2.6548	3.0542	3.3322	3.4430	4.0781	4.1773	4.6242	4.7389
	3	3.5920	3.7590	4.2012	4.2018	4.4615	4.8480	4.9709	5.5621	5.6187
F–C	0	0.8552	2.4002	2.9468	3.3076	3.7457	3.8887	4.3952	4.4361	4.8611
	1	0.2638	0.9304	1.9045	2.2904	2.7721	3.0750	3.2094	3.3176	3.8032
	2	2.1368	2.3814	2.7657	3.2293	3.6532	3.9018	4.3566	4.4829	4.5628
	3	3.2525	3.6288	3.8146	4.1908	4.5449	4.7364	5.1779	5.3807	5.8530
C–C	0	1.7192	3.0658	3.5340	4.0512	4.0879	4.1803	4.8290	5.0242	5.5558
	1	0.8980	1.7298	2.5722	2.7659	2.9806	3.4873	3.7056	3.8520	4.3108
	2	2.4586	2.7450	3.3803	3.5121	4.2108	4.2134	4.6585	4.7539	5.0998
	3	3.6727	3.8483	4.2671	4.4904	4.9127	5.0951	5.6633	5.7372	6.1127

shell with inner–outer ration $R_0/R_1=0.5$, length–radius ratio $L/R_1=2$ and $\mu=0.3$ is investigated. Assume that the shell is free at the edge $x=0$ whilst the edge $x=L$ is elastically restrained by only one group of spring components with various stiffnesses. For simplicity and convenience in the analysis, three stiffness parameters Γ_u, Γ_v and Γ_w, which are defined as the ratios of the corresponding spring stiffnesses to the flexural stiffness $D=Eh^3/\ 12(1-\mu^2)$, respectively, are introduced here (i.e. $\Gamma_u=\log_{10}(k_{uL}/D)$, $\Gamma_v=\log_{10}(k_{vL}/D)$ and $\Gamma_w=\log_{10}(k_{wL}/D)$). In Fig. 2, variation of the first and ninth modal ($n=2$, $m=1$, 9) frequency parameters $\Omega=\omega R_1\sqrt{p/G}$ of the considered cylindrical shell against the stiffness parameters Γ_u, Γ_v and Γ_w are depicted, respectively. From Fig. 2(a), it can be seen that the frequency parameters almost keep at a level when the stiffness parameter Γ_u is smaller than 0,

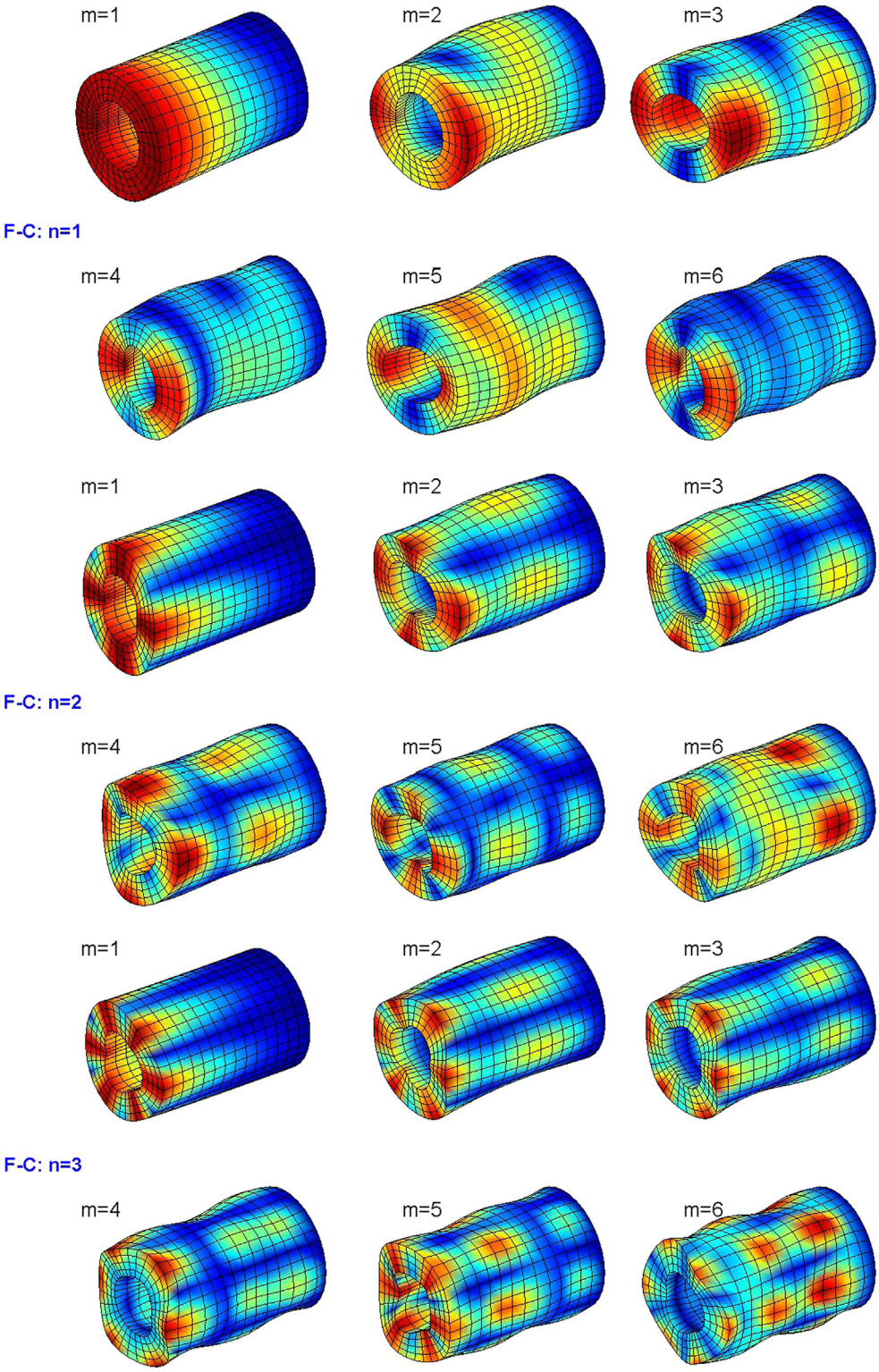

Fig. 3. Mode shapes of a cylindrical shell with F–C boundary conditions.

the change of the stiffness parameter has little effect on frequency parameters of the shell. As it further increase, a distinct influence can be observed, in which the frequency parameters increases rapidly, when it is beyond 4, the frequency parameters approach utmost and remain unchanged. The similar tendency can be seen when the shell is elastically restrained by the circumferential and radial springs, except that the active ranges of the stiffness parameters of the circumferential and radial boundary springs are shown as $[-1, 5]$ and $[-2, 3]$, see Fig. 2(b) and (c). Generally speaking, this study shows the active ranges of the boundary springs stiffness parameters (Γ_u, Γ_v and Γ_w) for the vibration frequencies of cylindrical shells are different. In this case, they can be defined as $[0, 4]$, $[-1, 5]$ and $[-2, 3]$, respectively.

In the following discussion, vibration frequencies and modal shapes of certain circular cylindrical shells with arbitrary classical end conditions and their combinations will be presented. Taking

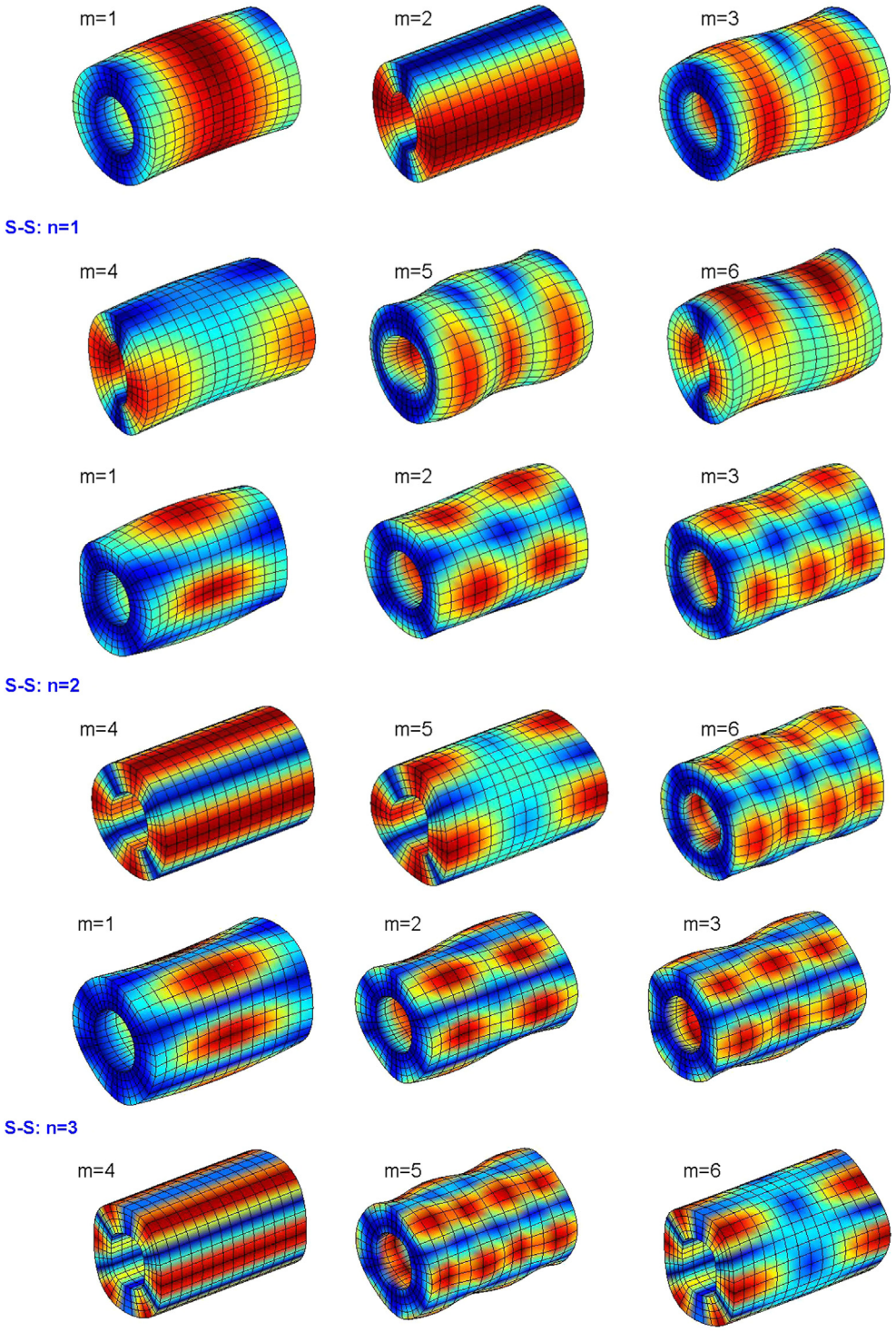

Fig. 4. Mode shapes of a cylindrical shell with S–S boundary conditions.

edge $x=0$ for example, the corresponding spring stiffness parameters for three types of classical end conditions which are commonly encountered in engineering practices are given as follows:

(1) Free edge (F): $\Gamma_u=\Gamma_v=\Gamma_w=0$;
(2) Simply supported edge (S): $\Gamma_u=0$, $\Gamma_v=\Gamma_w=7$;
(3) Clamped edge (C): $\Gamma_u=\Gamma_v=\Gamma_w=7$.

The appropriateness of defining the classical end conditions in terms of boundary spring parameters will be proved by several examples in later subsections. For the sake of simplicity, a two-letter string is applied to represent the end conditions of a cylindrical shell, such as C–F denotes a cylindrical shell subjected to clamped at end $x=0$ and free at end $x=L$.

3.2. Convergence and efficiency study

Theoretically, there are infinite terms in the modified Fourier series solution. However, the series is numerically truncated and only finite terms are counted in actual calculations. Thus, it is very important to check its accuracy, convergence and numerical robustness. Considering the circumferential symmetry of the circular shell, the convergence is checked in the axial and radial directions (i.e. x and r). In Table 1, the first ten ($m=1$–10) frequencies for a completely free thick cylindrical shell with seven truncation schemes (i.e. $M=Q=5$–11) are presented, in which two circumferential wave numbers ($n=1$, 2) are included. For convenience in expression, the dimensionless frequency parameter $\Omega=\omega R_1\sqrt{p/G}$ are applied in the analysis. The geometric and material constants of the shell are: inner–outer ration $R_0/R_1=0.5$, length–radius ratio $L/R_1=2$ and $\mu=0.3$. In all the following computations, the zero frequencies corresponding to the rigid body modes were omitted from the results. From Table 1, it is obvious that the modified Fourier series solution has an excellent convergence, and it is sufficiently accurate even when only a small number of terms are included in the series expression. The maximum difference in the tenth frequency between the 6×6-term solution and the 11×11-term one is less than 0.38%. Furthermore, by comparing with results published by Zhou et al. [19], we can find a very close agreement between these two results, although different displacement admissible functions and solution procedures were used in the literature. In order to further demonstrate the efficiency of the current method, convergence and comparison of the first nine frequency parameters $\Omega=2\omega R_1\sqrt{p/E}$ of a solid cylinder ($L/R_1=4$, $\mu=0.3$) with completely free boundary conditions are presented in Table 2. The solutions obtained by different types of truncation schemes are compared with those 3D results reported by Liew and Hung [32] using the Rayleigh–Ritz method based on polynomial functions. From the table, we can see that the present results are in excellent agreement with the referential data. The truncation terms of the method advocated by Liew and Huang [32] are smaller than the present ones. However, in Ref. [32], a specially customized set of beam functions are used as the displacement functions of the shell for each type of boundary conditions. The proposed method offers a unified solution for all the classical end conditions and the change of end conditions from one case to another is as easy as changing structural parameters without the need of making any change to the solution procedure. Moreover, from Table 3, where computational time versus number of modes (by the implicitly restarted Arnoldi algorithm) for a thick shell ($R_0/R_1=0.5$, $L/R_1=2$, $\mu=0.3$, $M\times Q=11\times11$) subjected to different boundary conditions is presented, we can see that the current modified Fourier series Ritz method is very efficient. The frequency results of the shell are calculated by the MATAB software on a laptop. The configuration of the computer is: Inter Core2 Duo CPU (2.1 GHz) and 2 GB RAM. Although the number of modes is as much as 40, the computing time is less than 1.423 s.

To further validate the accuracy and reliability of current solution, more numerical examples will be presented. In each case, the convergence study is performed and for brevity purposes, only the converged results are presented here.

3.3. Thick cylindrical shells with arbitrary classical ends

In this subsection, the present formulations are applied to study the free vibrations of thick cylindrical shells with arbitrary classical end conditions and their combinations. In Table 4, the natural frequencies which are expressed in terms of non-dimension parameters, $\Omega=\omega h/\pi\sqrt{\rho/G}$ of moderately thick isotropic S–S cylindrical shells are compared to those available in the literature for lower-mode numbers i.e. $n=1$, 2, 3 and $m=1$. Exact 3D elasticity results provided by Armenakas et al. [31] and Khalili et al. [23] are included in the comparison. Four kinds of length–radius ratios $L/R=2$, 1, 0.5, 0.25 are considered in the comparison

Table 8
Frequency parameters $\Omega=\omega R_1\sqrt{p/G}$ for a circular cylindrical shell with various end conditions and thickness–radius ratios ($L/R_1=2$, $\mu=0.3$, $K_r=0$, $K_g=0$).

h/R_1	n	F–F			S–S			C–C		
		$m=1$	$m=2$	$m=3$	$m=1$	$m=2$	$m=3$	$m=1$	$m=2$	$m=3$
0.05	1	1.2672	1.4412	1.6177	0.9719	1.0258	1.4737	1.0060	1.5069	1.7332
	2	0.0683	0.0902	1.0210	0.5614	1.1513	1.4972	0.6725	1.2036	1.5878
	3	0.1926	0.2275	0.7448	0.4058	0.9157	1.3480	0.5318	1.0001	1.4579
0.15	1	1.3227	1.5364	1.9623	0.9859	1.0823	1.6553	1.0691	1.8234	2.5040
	2	0.2237	0.2851	1.1892	0.6533	1.4293	2.1644	0.8332	1.6270	2.5060
	3	0.6198	0.7129	1.2392	0.8306	1.4833	2.3242	0.9710	1.6926	2.6142
0.25	1	1.3864	1.6529	2.2547	1.0069	1.1467	1.8896	1.1469	2.1524	2.6702
	2	0.4050	0.4944	1.4251	0.8198	1.7896	2.2925	1.0491	2.0479	3.2003
	3	1.0837	1.2080	1.7891	1.3328	2.1124	3.2015	1.4760	2.3379	3.4729
0.35	1	1.4617	1.7662	2.3293	1.0319	1.2207	2.1156	1.2213	2.3901	2.7076
	2	0.6119	0.7116	1.6544	1.0235	2.1236	2.4374	1.2708	2.3586	3.3272
	3	1.5619	1.6855	2.2606	1.8271	2.6557	3.6460	1.9614	2.8435	4.0345
0.45	1	1.5521	1.8581	2.4239	1.0583	1.3066	2.3073	1.2835	2.5262	2.7783
	2	0.8441	0.9330	1.8501	1.2430	2.4048	2.5977	1.4877	2.5824	3.4796
	3	2.0444	2.1351	2.6422	2.2989	3.1127	3.8596	2.4241	3.2561	4.4263

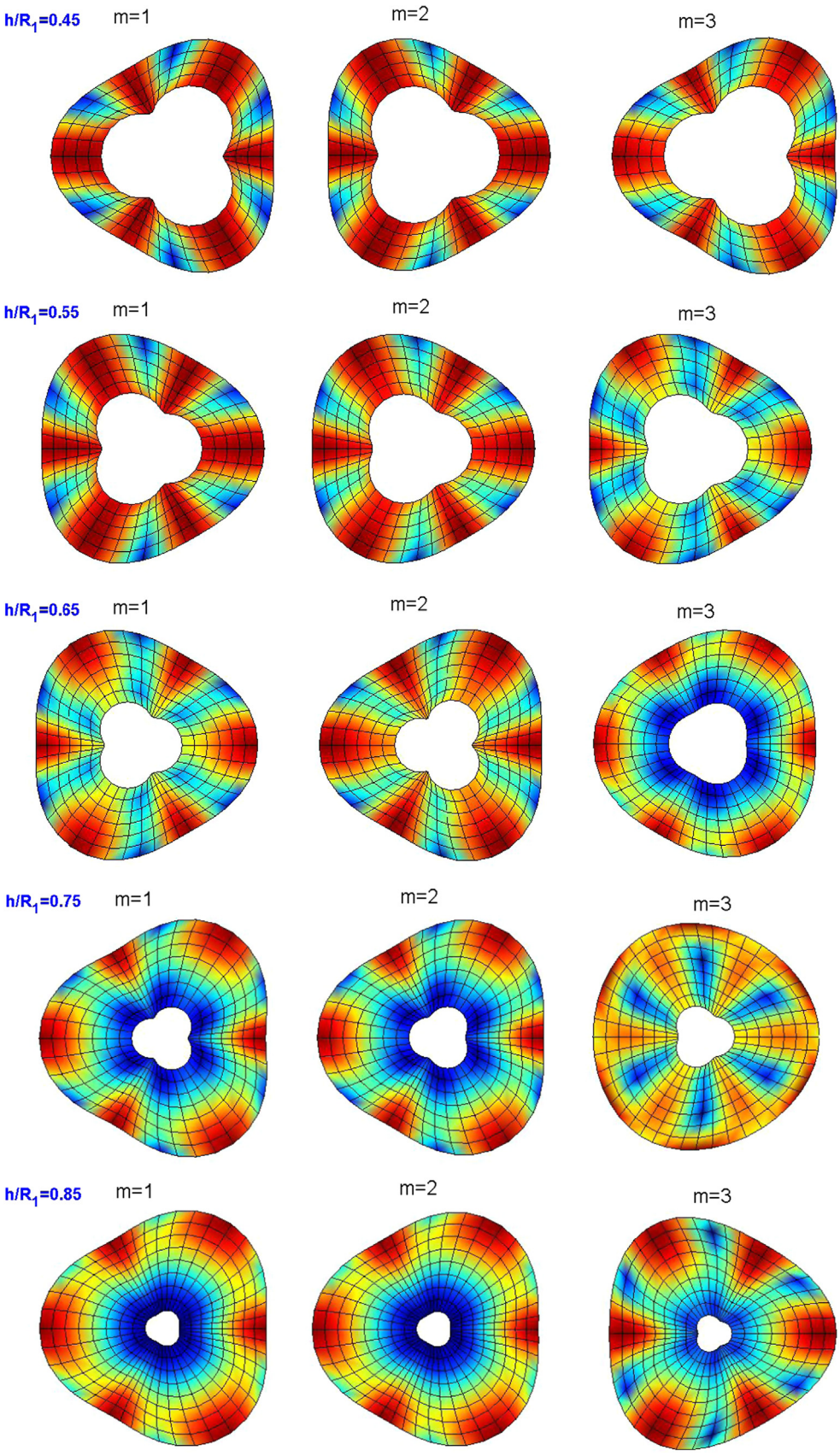

Fig. 5. Some selected mode shapes (F–F, $n=3$, $m=1$–3) in the end $x=0$ of a thick shell with various thicknesses.

as well. The geometric and material constants of the shell are: $h/R=0.1$, $\mu=0.3$. From the table, we can see that the present results agree well with the referential data. The discrepancy is very small and does not exceed 1.11% for the worst case. The small discrepancy may be attributed to the different solution approaches were used in the literature. Furthermore, it can be seen from the table that the frequency parameters of the shells increase with length–radius ratio L/R decrease.

For the sake of completeness, in Table 5, the first three modal ($m=1$–3) frequency parameters $\Omega=\omega L\sqrt{\rho(1+\mu)/E}$ for a thick cylindrical shell subjected to F–F, C–F and C–C end conditions are compared to exact 3D elasticity results provided by Malekzadeh et al. [36] based on LW-DQ and FEM methods. Five circumferential wave numbers ($n=1$–5) are included in the comparison. The geometric and material properties of the considered shell are given as: $h/R=0.3$, $L/R=1$ and $\mu=0.3$. Through comprising, it is obvious that the present solutions match very well with results given by Malekzadeh et al. [36]. The small deviations in the results are caused by different computation methods were used in the literature.

The excellent agreements of comparisons between the proposed solutions and the published results for cylindrical shells with F–F, S–S, C–C and C–F end conditions separately given in Tables 1 and 2 and Tables 4 and 5 indicate that the present analysis is accurate. Having gained confidence in present method, some further numerical results are given in the following presentation.

In Tables 6 and 7, the first nine modal ($m=1$–9, $n=0$–3) frequency parameters $\Omega=\omega R_1\sqrt{\rho/G}$ of a circular cylindrical shell subjected to five different classical end combinations (i.e. F–F, F–S, S–S, F–C and C–C) are presented, respectively. The material parameters and geometric constants of the investigated shells are: $L/R_1=3$, $\mu=0.3$ $R_0/R_1=0.5$ or $R_0/R_1=0$ (solid). It is shown that the frequency parameters of the shells increase with the boundary restraints get rigid and the frequency parameters for the solid cylinder are higher than the hollow one. In fact, from Eq. (21), the eigenfrequencies and eigenvectors are simultaneously obtained. For each eigenfrequency, the corresponding eigenvector contains entire expanded and supplemented coefficients. By substituting the eigenvector into the admissible displacement functions (Eq. (12)), the corresponding modal shape of the considered shell can be easily determined. In Figs. 3 and 4, the corresponding modal shapes for the lowest six longitudinal modal frequencies given in Table 6 that the considered cylindrical shell with F–C and S–S boundary conditions are plotted, respectively. From the figures, the vibration behaviors of the shell can be seen vividly.

Then let us look into the influence of thickness–radius ratio h/R_1 on natural frequencies of cylindrical shells with various end conditions. In Table 8, the first three modal ($m=1$–3) frequencies which are expressed in terms of dimensionless parameters, $\Omega=\omega R_1\sqrt{\rho/G}$ of a circular cylindrical subjected to F–F, S–S and C–C end conditions and different thickness–radius ratios are given, in which three circumferential wave numbers ($n=1$–3) are included. Five different thickness–radius ratios considered in the analysis are: $h/R_1=0.05$, 0.15, 0.25, 0.35 and 0.45. Form Table 8, it can be seen that the frequency parameters of the shell monotonically increase as the thickness–radius ratio increases. In Fig. 5, some selected mode shapes (F–F, $n=3$, $m=1$–3) in the end $x=0$ of the thick shell with various thicknesses are presented.

The above numerical examples are presented as circular cylindrical shells with arbitrary classical end conditions and their combinations. It is obvious that the frequency parameters and modal shapes of the circular cylindrical shells subjected to general end conditions and their combinations can be determined easily by the modified Fourier series method. In the next section, our work will focus on thick cylindrical shells resting on elastic foundations with general end conditions

3.4. Thick cylindrical shells resting on elastic foundations

As we know, a variety of possible elastic foundation support cases such as cylindrical shells completely or partly placed in (or laid on) a soil medium are usually encountered in engineering applications and the vibration analyses of these shells with such boundary conditions

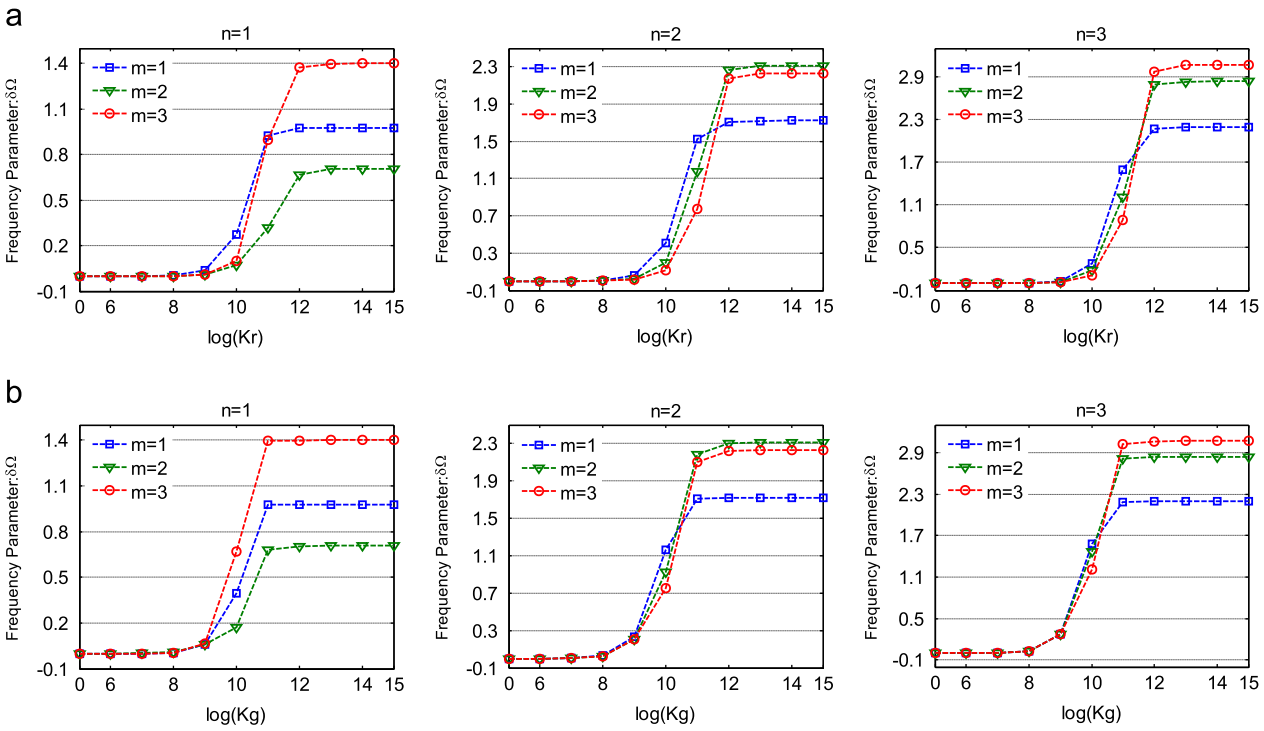

Fig. 6. Variation of frequency parameters $\delta\Omega$ versus foundation coefficients for a moderately thick cylindrical shell with C–F end condition: (a) K_r ($K_g=0$); (b) K_g ($K_r=0$).

are necessary and of great significance. Thus, in this part, the present formulations are used to investigate the free vibration behaviors of thick cylindrical shells resting on elastic foundations with arbitrary end conditions. Unless otherwise stated, the material and geometric constants of the shell considered in the following discussion are: $L/R_1=2$, $R_0/R_1=0.8$ and $\mu=0.3$.

First, let us consider the effects of variation of foundation coefficients on the frequencies of the considered cylindrical shell with different end conditions. For simplicity and convenience in the analysis, frequency parameters $\delta\Omega$ which are defined as the differences of the corresponding non-dimensional frequency parameters $\Omega=\omega R_1\sqrt{p/G}$ to those of the foundation coefficients equal to zero (i.e.$\delta\Omega=\Omega_{|K_r,K_g}-\Omega_{|K_r=0,K_g=0}$) are introduced here. In Fig. 6(a), the variation of the lowest three longitudinal modal ($m=1, 2, 3$) frequency parameters $\delta\Omega$ of the considered shell with C–F end condition against the foundation coefficient K_r ($K_g=0$) are depicted. It is clear that there is little variation in frequency parameters $\delta\Omega$ as the value of the foundation coefficient Kr increasing from 0 to 10^8 N/m. As it further increase, a distinct influence can be observed, in which the frequency parameters increases rapidly, when K_r is bigger than 10^{13} N/m, the frequency parameters $\delta\Omega$ approach their utmost and remain unchanged. In Fig. 6(b), the variation of the lowest three modal ($m=1, 2, 3$) frequency parameters $\delta\Omega$ against the other foundation coefficient K_g ($K_r=0$) are presented. The variation traces of the frequency parameter $\delta\Omega$ are similar to Fig. 6(a). In Fig. 7, the variation of the frequency parameters $\delta\Omega$ against the foundation coefficient K_r and K_g for the shell subjected to C–C end condition are presented, respectively. Comparing Figs. 6 and 7, it can be seen that influence of the foundation coefficients on the frequency parameters of the shell varying with circumference numbers and end conditions as well. In addition, increase of the stiffness of the foundation causes the frequency parameters to increase.

Then, let us look into the shell resting on an elastic foundation with one coefficient equal to infinite. In Table 9, the first three ($n=1, 2, 3$, $m=1, 2, 3$) modal frequency parameters $\Omega=\omega R_1\sqrt{p/G}$ for the circular cylindrical shell resting on elastic foundation with one coefficient equal to infinite (assigned as 10^{14} N/m or N/rad) and the other one change from 0 to extremely large (assigned as 10^{14} N/m or N/rad) are presented. Two different end conditions included in the computations are C–F and C–C. In the table, it can be seen that the varying of the coefficient has little effect on frequency parameters of the shell and the shell is thought to be rigidly restrained in the out surface in such case. At last, some further numerical results for cylindrical shells subjected to different kinds of end conditions are given in the following presentation. In Table 10, the first three ($m=1$–3) frequency parameters $\Omega=\omega R_1\sqrt{p/G}$ for the first five circumferential wave numbers ($n=1$–5) of the circular cylindrical shell subjected to three different classical end conditions (i.e. F–F, S–S, and C–C) resting on elastic foundations are presented. It is shown that the frequency parameters of the shells increase with the boundary restraints get more rigid.

Table 9
Frequency parameters $\Omega=\omega R_1\sqrt{p/G}$ for a cylindrical shell with C–F and C–C end conditions and different foundation coefficients ($L/R_1=2$, $R_0/R_1=0.8$, $\mu=0.3$).

n	m	C–F, $K_g=10^{14}$		C–F, $K_r=10^{14}$		C–C, $K_g=10^{14}$		C–C, $K_r=10^{14}$	
		$K_r=0$	$K_r=10^{14}$	$K_g=0$	$K_g=10^{14}$	K_r 0	$K_r=10^{14}$	$K_g=0$	$K_g=10^{14}$
1	1	1.4527	1.4527	1.4527	1.4527	2.4197	2.4197	2.4196	2.4197
	2	1.9757	1.9757	1.9757	1.9757	2.6552	2.6552	2.6551	2.6552
	3	3.0667	3.0667	3.0667	3.0667	3.8115	3.8115	3.8115	3.8115
2	1	2.1456	2.1456	2.1456	2.1456	3.0836	3.0836	3.0836	3.0836
	2	3.3763	3.3763	3.3763	3.3763	3.8654	3.8654	3.8653	3.8654
	3	4.2383	4.2383	4.2383	4.2383	4.9399	4.9399	4.9398	4.9399
3	1	3.0948	3.0948	3.0947	3.0948	3.8738	3.8738	3.8738	3.8738
	2	4.1871	4.1871	4.1871	4.1871	4.9159	4.9159	4.9158	4.9159
	3	5.2828	5.2828	5.2827	5.2828	6.0078	6.0078	6.0078	6.0078

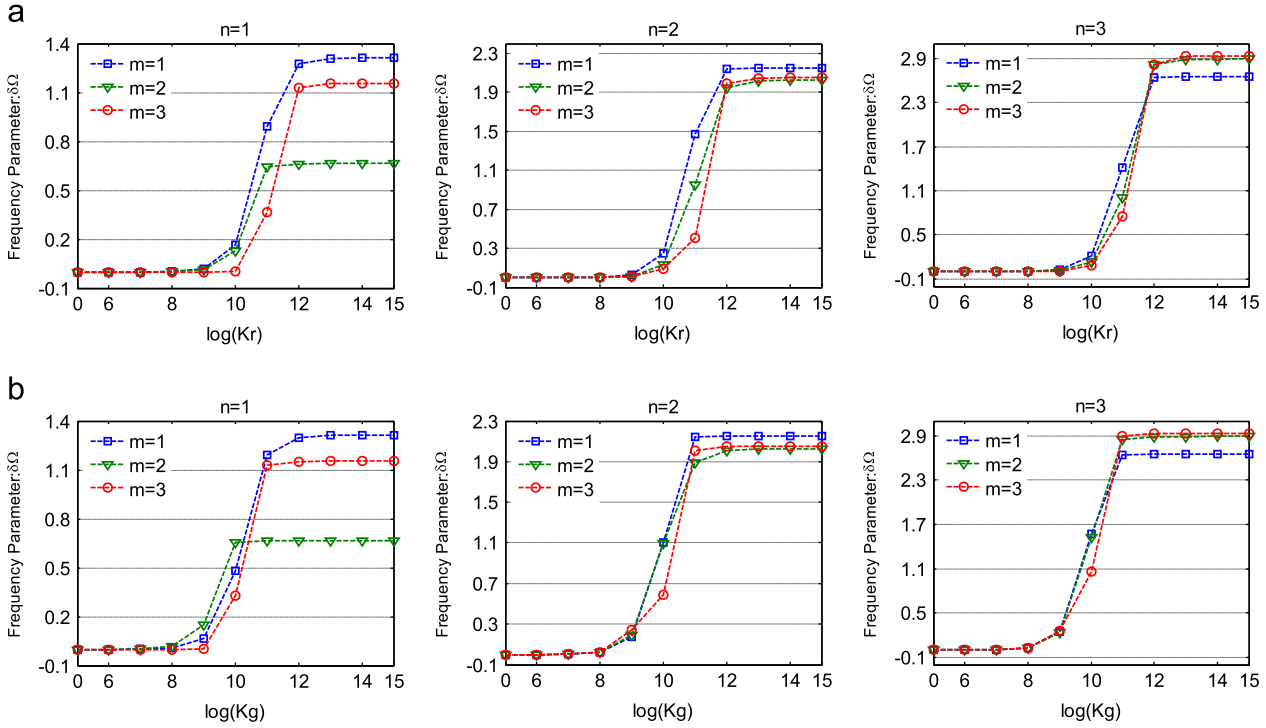

Fig. 7. Variation of frequency parameters $\delta\Omega$ versus foundation coefficients for a moderately thick cylindrical shell with C–C end condition: (a) K_r ($K_g=0$); (b) K_g ($K_r=0$).

Table 10
Frequency parameters $\Omega=\omega R_1\sqrt{p/G}$ for a cylindrical shell with various end conditions and foundation coefficients ($L/R_1=2$, $R_0/R_1=0.8$, $\mu=0.3$).

Foundation coefficients	n	F–F			S–S			C–C		
		$m=1$	$m=2$	$m=3$	$m=1$	$m=2$	$m=3$	$m=1$	$m=2$	$m=3$
$K_r=1\times10^{11}$	1	0.6622	1.3880	2.0953	1.1134	1.7210	2.7904	1.9960	2.6355	3.0244
$K_g=0$	2	1.6625	2.1439	2.3693	2.1459	2.2265	2.7323	2.4027	2.7938	3.2987
	3	2.4174	2.4976	2.6214	2.5181	2.8906	3.3390	2.6406	3.0358	3.8288
	4	2.8463	2.8790	3.0828	2.9193	3.2670	3.9530	2.9880	3.4085	4.1587
	5	3.3626	3.4297	3.6906	3.4735	3.8298	4.4894	3.5174	3.9449	4.6610
$K_r=0$	1	0.7263	1.3891	2.3503	1.1134	1.8657	3.2382	2.3026	2.6554	3.7891
$K_g=1\times10^{11}$	2	1.8424	2.5473	3.5700	2.2265	2.6688	3.8017	3.0786	3.7335	4.9035
	3	2.9483	3.2873	4.5104	3.3390	3.6543	4.5274	3.8666	4.8723	5.9786
	4	4.0236	4.1854	5.3027	4.4507	4.6957	5.3931	4.8171	5.6987	6.8038
	5	5.0762	5.1536	6.1742	5.5613	5.7610	6.3375	5.8376	6.5671	7.5720

4. Conclusions

A unified 3D elasticity method has been developed for the free vibration analysis of circular cylindrical shells subjected to general end conditions and resting on elastic foundations. The energy variational principle is employed to derive the formulation based on the 3D elasticity theory. Each of the shell displacements, regardless of boundary conditions, is constructed as a standard Fourier cosine series supplemented with several auxiliary functions introduced to eliminate all the possible discontinuities with the original displacement and its derivatives throughout the entire shell space including the boundaries at the edges and accelerate the convergence of series representations. The efficiency, accuracy and reliability of present method are illustrated for free vibration analysis of moderately thick and thick circular cylindrical shells with different end conditions, with respect to various parameters such as the length–radius ratio and the inside–outside radius ratio. Numerical results produced by proposed method are found in excellent agreement with those available in open literature. The method described in this paper is believed to include several advantages: first, it is a unified 3D elasticity method which can be used to predict the natural vibration characteristics of thick circular cylindrical shells subjected to arbitrary end conditions and elastic foundation supports accurately; second, the proposed method offers an easy analysis operation for the entire restraining conditions and the change of end conditions from one case to another is as easy as changing structure parameters without the need of making any change to the solution procedure; finally, new results for different foundation coefficients with various end conditions are presented, which may serve as benchmark solutions.

Acknowledgments

The authors would like to thank the reviewers for their Constructive comments. The authors gratefully acknowledge the financial support from the National Natural Science Foundation of China (Nos. 51175098, 51279035 and 10802024).

Appendix A. Detailed expressions for the stiffness matrix K and mass matrix M

The detailed expressions of the stiffness and mass matrixes in Eq. (21) are given as follows. To make the expressions simple and clear, six indexes are pre-defined:

$$e=q+(Q+1)*m+1,\quad f=m+(M+1)*(l-1)+1$$

$$e'=q'+(Q+1)*m'+1,\quad f'=m'+(M+1)*(l'-1)+1$$

$$g=q+(Q+1)*(l-1)+1\quad g'=q'+(Q+1)*(l'-1)+1$$

The elements in the stiffness matrix **K** are calculated according to the following formulations:

$$\{\mathbf{K}_{1,1}\}_{e,e'}=\frac{E}{1-\mu^2}C_{cc}^{11}D_{cc}^{001}E_{cc}^{00}+\frac{E}{2(1+\mu)}(C_{cc}^{00}D_{cc}^{111}E_{cc}^{00}+C_{cc}^{11}D_{cc}^{00-1}E_{cc}^{11})+[k_{u0}+k_{uL}(-1)^{m+m'}]D_{cc}^{001}E_{cc}^{00}$$

$$\{\mathbf{K}_{1,2}\}_{f,e'}=\frac{E}{1-\mu^2}C_{cc}^{11}D_{\zeta c}^{001}E_{cc}^{00}+\frac{E}{2(1+\mu)}(C_{cc}^{00}D_{\zeta c}^{111}E_{cc}^{00}+C_{cc}^{11}D_{\zeta c}^{00-1}E_{cc}^{11})+[k_{u0}+k_{uL}(-1)^{m+m'}]D_{\zeta c}^{001}E_{cc}^{00}$$

$$\{\mathbf{K}_{1,3}\}_{g,e'}=\frac{E}{1-\mu^2}C_{\zeta c}^{11}D_{cc}^{001}E_{cc}^{00}+\frac{E}{2(1+\mu)}(C_{\zeta c}^{00}D_{cc}^{111}E_{cc}^{00}+C_{\zeta c}^{11}D_{cc}^{00-1}E_{cc}^{11})$$

$$\{\mathbf{K}_{1,4}\}_{e,e'}=\frac{\mu E_2}{1-\mu^2}C_{cc}^{01}D_{cc}^{000}E_{sc}^{10}+\frac{E}{2(1+\mu)}C_{cc}^{10}D_{cc}^{000}E_{sc}^{01}$$

$$\{\mathbf{K}_{1,5}\}_{f,e'}=\frac{\mu E_2}{1-\mu^2}C_{cc}^{01}D_{\zeta c}^{000}E_{sc}^{10}+\frac{E}{2(1+\mu)}C_{cc}^{10}D_{\zeta c}^{000}E_{sc}^{01}$$

$$\{\mathbf{K}_{1,6}\}_{g,e'}=\frac{\mu E_2}{1-\mu^2}C_{\zeta c}^{01}D_{cc}^{000}E_{sc}^{10}+\frac{E}{2(1+\mu)}C_{\zeta c}^{10}D_{cc}^{000}E_{sc}^{01}$$

$$\{\mathbf{K}_{1,7}\}_{e,e'}=\frac{\mu E_2}{1-\mu^2}(C_{cc}^{01}D_{cc}^{000}E_{cc}^{00}+C_{cc}^{01}D_{cc}^{101}E_{cc}^{00})+\frac{E}{2(1+\mu)}C_{cc}^{10}D_{cc}^{011}E_{cc}^{00}$$

$$\{\mathbf{K}_{1,8}\}_{f,e'}=\frac{\mu E_2}{1-\mu^2}(C_{cc}^{01}D_{\zeta c}^{000}E_{cc}^{00}+C_{cc}^{01}D_{\zeta c}^{101}E_{cc}^{00})+\frac{E}{2(1+\mu)}C_{cc}^{10}D_{\zeta c}^{011}E_{cc}^{00}$$

$$\{\mathbf{K}_{1,9}\}_{g,e'}=\frac{\mu E_2}{1-\mu^2}(C_{\zeta c}^{01}D_{cc}^{000}E_{cc}^{00}+C_{\zeta c}^{01}D_{cc}^{101}E_{cc}^{00})+\frac{E}{2(1+\mu)}C_{\zeta c}^{10}D_{cc}^{011}E_{cc}^{00}$$

$$\{\mathbf{K}_{2,2}\}_{f,f'}=\frac{E}{1-\mu^2}C_{cc}^{11}D_{\zeta\zeta}^{001}E_{cc}^{00}+\frac{E}{2(1+\mu)}(C_{cc}^{00}D_{\zeta\zeta}^{111}E_{cc}^{00}+C_{cc}^{11}D_{\zeta\zeta}^{00-1}E_{cc}^{11})+[k_{u0}+k_{uL}(-1)^{m+m'}]D_{\zeta\zeta}^{001}E_{cc}^{00}$$

$$\{\mathbf{K}_{2,3}\}_{g,f'}=\frac{E}{1-\mu^2}C_{\zeta c}^{11}D_{c\zeta}^{001}E_{cc}^{00}+\frac{E}{2(1+\mu)}(C_{\zeta c}^{00}D_{c\zeta}^{111}E_{cc}^{00}+C_{\zeta c}^{11}D_{c\zeta}^{00-1}E_{cc}^{11})$$

$$\{\mathbf{K}_{2,4}\}_{e,f'}=\frac{\mu E_2}{1-\mu^2}C_{cc}^{01}D_{c\zeta}^{000}E_{sc}^{10}+\frac{E}{2(1+\mu)}C_{cc}^{10}D_{c\zeta}^{000}E_{sc}^{01}$$

$$\{\mathbf{K}_{2,5}\}_{f,f'}=\frac{\mu E_2}{1-\mu^2}C_{cc}^{01}D_{\zeta\zeta}^{000}E_{sc}^{10}+\frac{E}{2(1+\mu)}C_{cc}^{10}D_{\zeta\zeta}^{000}E_{sc}^{01}$$

$$\{\mathbf{K}_{2,6}\}_{g,f'}=\frac{\mu E_2}{1-\mu^2}C_{\zeta c}^{01}D_{c\zeta}^{000}E_{sc}^{10}+\frac{E}{2(1+\mu)}C_{\zeta c}^{10}D_{c\zeta}^{000}E_{sc}^{01}$$

$$\{\mathbf{K}_{2,7}\}_{e,f'}=\frac{\mu E_2}{1-\mu^2}(C_{cc}^{01}D_{c\zeta}^{000}E_{cc}^{00}+C_{cc}^{01}D_{c\zeta}^{101}E_{cc}^{00})+\frac{E}{2(1+\mu)}C_{cc}^{10}D_{c\zeta}^{011}E_{cc}^{00}$$

$$\{\mathbf{K}_{2,8}\}_{f,f'}=\frac{\mu E_2}{1-\mu^2}(C_{cc}^{01}D_{\zeta\zeta}^{000}E_{cc}^{00}+C_{cc}^{01}D_{\zeta\zeta}^{101}E_{cc}^{00})+\frac{E}{2(1+\mu)}C_{cc}^{10}D_{\zeta\zeta}^{011}E_{cc}^{00}$$

$$\{\mathbf{K}_{2,9}\}_{g,f'}=\frac{\mu E_2}{1-\mu^2}(C_{\zeta c}^{01}D_{c\zeta}^{000}E_{cc}^{00}+C_{\zeta c}^{01}D_{c\zeta}^{101}E_{cc}^{00})+\frac{E}{2(1+\mu)}C_{\zeta c}^{10}D_{c\zeta}^{011}E_{cc}^{00}$$

$$\{\mathbf{K}_{3,3}\}_{g,g'}=\frac{E}{1-\mu^2}C_{\zeta\zeta}^{11}D_{cc}^{001}E_{cc}^{00}+\frac{E}{2(1+\mu)}(C_{\zeta\zeta}^{00}D_{cc}^{111}E_{cc}^{00}+C_{\zeta\zeta}^{11}D_{cc}^{00-1}E_{cc}^{11})$$

$$\{\mathbf{K}_{3,4}\}_{e,g'}=\frac{\mu E_2}{1-\mu^2}C_{c\zeta}^{01}D_{cc}^{000}E_{sc}^{10}+\frac{E}{2(1+\mu)}C_{c\zeta}^{10}D_{cc}^{000}E_{sc}^{01}$$

$$\{\mathbf{K}_{3,5}\}_{f,g'}=\frac{\mu E_2}{1-\mu^2}C_{c\zeta}^{01}D_{\zeta c}^{000}E_{sc}^{10}+\frac{E}{2(1+\mu)}C_{c\zeta}^{10}D_{\zeta c}^{000}E_{sc}^{01}$$

$$\{\mathbf{K}_{3,6}\}_{g,g'}=\frac{\mu E_2}{1-\mu^2}C_{\zeta\zeta}^{01}D_{cc}^{000}E_{sc}^{10}+\frac{E}{2(1+\mu)}C_{\zeta\zeta}^{10}D_{cc}^{000}E_{sc}^{01}$$

$$\{\mathbf{K}_{3,7}\}_{e,g'}=\frac{\mu E_2}{1-\mu^2}(C_{c\zeta}^{01}D_{cc}^{000}E_{cc}^{00}+C_{c\zeta}^{01}D_{cc}^{101}E_{cc}^{00})+\frac{E}{2(1+\mu)}C_{c\zeta}^{10}D_{cc}^{011}E_{cc}^{00}$$

$$\{\mathbf{K}_{3,8}\}_{f,g'}=\frac{\mu E_2}{1-\mu^2}(C_{c\zeta}^{01}D_{\zeta c}^{000}E_{cc}^{00}+C_{c\zeta}^{01}D_{\zeta c}^{101}E_{cc}^{00})+\frac{E}{2(1+\mu)}C_{c\zeta}^{10}D_{\zeta c}^{011}E_{cc}^{00}$$

$$\{\mathbf{K}_{3,9}\}_{g,g'}=\frac{\mu E_2}{1-\mu^2}(C_{\zeta\zeta}^{01}D_{cc}^{000}E_{cc}^{00}+C_{\zeta\zeta}^{01}D_{cc}^{101}E_{cc}^{00})+\frac{E}{2(1+\mu)}C_{\zeta\zeta}^{10}D_{cc}^{011}E_{cc}^{00}$$

$$\{\mathbf{K}_{4,4}\}_{e,e'}=\frac{E}{1-\mu^2}C_{cc}^{00}D_{cc}^{00-1}E_{ss}^{11}+\frac{E}{2(1+\mu)}C_{cc}^{00}E_{ss}^{00}(D_{cc}^{111}-D_{cc}^{010}-D_{cc}^{100}+D_{cc}^{00-1})+\frac{E}{2(1+\mu)}C_{cc}^{11}D_{cc}^{001}E_{ss}^{00}+[k_{v0}+k_{vL}(-1)^{m+m'}]D_{cc}^{001}E_{ss}^{00}$$

$$\{\mathbf{K}_{4,5}\}_{f,e'}=\frac{E}{1-\mu^2}C_{cc}^{00}D_{\zeta c}^{00-1}E_{ss}^{11}+\frac{E}{2(1+\mu)}C_{cc}^{00}E_{ss}^{00}(D_{\zeta c}^{111}-D_{\zeta c}^{010}-D_{\zeta c}^{100}+D_{\zeta c}^{00-1})+\frac{E}{2(1+\mu)}C_{cc}^{11}D_{\zeta c}^{001}E_{ss}^{00}+[k_{v0}+k_{vL}(-1)^{m+m'}]D_{\zeta c}^{001}E_{ss}^{00}$$

$$\{\mathbf{K}_{4,6}\}_{g,e'}=\frac{E}{1-\mu^2}C_{\zeta c}^{00}D_{cc}^{00-1}E_{ss}^{11}+\frac{E}{2(1+\mu)}C_{\zeta c}^{00}E_{ss}^{00}(D_{cc}^{111}-D_{cc}^{010}-D_{cc}^{100}+D_{cc}^{00-1})+\frac{E}{2(1+\mu)}C_{\zeta c}^{11}D_{cc}^{001}E_{ss}^{00}$$

$$\{\mathbf{K}_{4,7}\}_{e,e'}=\frac{E}{1-\mu^2}C_{cc}^{00}D_{cc}^{00-1}E_{cs}^{01}+\frac{\mu E_2}{1-\mu^2}C_{cc}^{00}D_{cc}^{100}E_{cs}^{01}+\frac{E}{2(1+\mu)}C_{cc}^{00}E_{cs}^{10}(D_{cc}^{010}-D_{cc}^{00-1})$$

$$\{\mathbf{K}_{4,8}\}_{f,e'}=\frac{E}{1-\mu^2}C_{cc}^{00}D_{\zeta c}^{00-1}E_{cs}^{01}+\frac{\mu E_2}{1-\mu^2}C_{cc}^{00}D_{\zeta c}^{100}E_{cs}^{01}+\frac{E}{2(1+\mu)}C_{cc}^{00}E_{cs}^{10}(D_{\zeta c}^{010}-D_{\zeta c}^{00-1})$$

$$\{\mathbf{K}_{4,9}\}_{g,e'}=\frac{E}{1-\mu^2}C_{\zeta c}^{00}D_{cc}^{00-1}E_{cs}^{01}+\frac{\mu E_2}{1-\mu^2}C_{\zeta c}^{00}D_{cc}^{100}E_{cs}^{01}+\frac{E}{2(1+\mu)}C_{\zeta c}^{00}E_{cs}^{10}(D_{cc}^{010}-D_{cc}^{00-1})$$

$$\{\mathbf{K}_{5,5}\}_{f,f'}=\frac{E}{1-\mu^2}C_{cc}^{00}D_{\zeta\zeta}^{00-1}E_{ss}^{11}+\frac{E}{2(1+\mu)}C_{cc}^{00}E_{ss}^{00}(D_{\zeta\zeta}^{111}-D_{\zeta\zeta}^{010}-D_{\zeta\zeta}^{100}+D_{\zeta\zeta}^{00-1})+\frac{E}{2(1+\mu)}C_{cc}^{11}D_{\zeta\zeta}^{001}E_{ss}^{00}+[k_{v0}+k_{vL}(-1)^{m+m'}]D_{\zeta\zeta}^{001}E_{ss}^{00}$$

$$\{\mathbf{K}_{5,6}\}_{g,f'}=\frac{E}{1-\mu^2}C_{\zeta c}^{00}D_{c\zeta}^{00-1}E_{ss}^{11}+\frac{E}{2(1+\mu)}C_{\zeta c}^{00}E_{ss}^{00}(D_{c\zeta}^{111}-D_{c\zeta}^{010}-D_{c\zeta}^{100}+D_{c\zeta}^{00-1})+\frac{E}{2(1+\mu)}C_{\zeta c}^{11}D_{c\zeta}^{001}E_{ss}^{00}$$

$$\{\mathbf{K}_{5,7}\}_{e,f'}=\frac{E}{1-\mu^2}C_{cc}^{00}D_{c\zeta}^{00-1}E_{cs}^{01}+\frac{\mu E_2}{1-\mu^2}C_{cc}^{00}D_{c\zeta}^{100}E_{cs}^{01}+\frac{E}{2(1+\mu)}C_{cc}^{00}E_{cs}^{10}(D_{c\zeta}^{010}-D_{c\zeta}^{00-1})$$

$$\{\mathbf{K}_{5,8}\}_{f,f'}=\frac{E}{1-\mu^2}C_{cc}^{00}D_{\zeta\zeta}^{00-1}E_{cs}^{01}+\frac{\mu E_2}{1-\mu^2}C_{cc}^{00}D_{\zeta\zeta}^{100}E_{cs}^{01}+\frac{E}{2(1+\mu)}C_{cc}^{00}E_{cs}^{10}(D_{\zeta\zeta}^{010}-D_{\zeta\zeta}^{00-1})$$

$$\{\mathbf{K}_{5,9}\}_{g,f'}=\frac{E}{1-\mu^2}C_{\zeta c}^{00}D_{c\zeta}^{00-1}E_{cs}^{01}+\frac{\mu E_2}{1-\mu^2}C_{\zeta c}^{00}D_{c\zeta}^{100}E_{cs}^{01}+\frac{E}{2(1+\mu)}C_{\zeta c}^{00}E_{cs}^{10}(D_{c\zeta}^{010}-D_{c\zeta}^{00-1})$$

$$\{\mathbf{K}_{6,6}\}_{g,g'}=\frac{E}{1-\mu^2}C_{\zeta\zeta}^{00}D_{cc}^{00-1}E_{ss}^{11}+\frac{E}{2(1+\mu)}C_{\zeta\zeta}^{00}E_{ss}^{00}(D_{cc}^{111}-D_{cc}^{010}-D_{cc}^{100}+D_{cc}^{00-1})+\frac{E}{2(1+\mu)}C_{\zeta\zeta}^{11}D_{cc}^{001}E_{ss}^{00}$$

$$\{\mathbf{K}_{6,7}\}_{e,g'}=\frac{E}{1-\mu^2}C_{c\zeta}^{00}D_{cc}^{00-1}E_{cs}^{01}+\frac{\mu E_2}{1-\mu^2}C_{c\zeta}^{00}D_{cc}^{100}E_{cs}^{01}+\frac{E}{2(1+\mu)}C_{c\zeta}^{00}E_{cs}^{10}(D_{cc}^{010}-D_{cc}^{00-1})$$

$$\{\mathbf{K}_{6,8}\}_{f,g'}=\frac{E}{1-\mu^2}C_{c\zeta}^{00}D_{\zeta c}^{00-1}E_{cs}^{01}+\frac{\mu E_2}{1-\mu^2}C_{c\zeta}^{00}D_{\zeta c}^{100}E_{cs}^{01}+\frac{E}{2(1+\mu)}C_{c\zeta}^{00}E_{cs}^{10}(D_{\zeta c}^{010}-D_{\zeta c}^{00-1})$$

$$\{\mathbf{K}_{6,9}\}_{g,g'}=\frac{E}{1-\mu^2}C_{\zeta\zeta}^{00}D_{cc}^{00-1}E_{cs}^{01}+\frac{\mu E_2}{1-\mu^2}C_{\zeta\zeta}^{00}D_{cc}^{100}E_{cs}^{01}+\frac{E}{2(1+\mu)}C_{\zeta\zeta}^{00}E_{cs}^{10}(D_{cc}^{010}-D_{cc}^{00-1})$$

$$\{\mathbf{K}_{7,7}\}_{e,e'}=\frac{E}{1-\mu^2}C_{cc}^{00}E_{cc}^{00}[D_{cc}^{00-1}+D_{cc}^{111}]+\frac{\mu E_2}{1-\mu^2}C_{cc}^{00}E_{cc}^{00}[D_{cc}^{010}+D_{cc}^{100}]+\frac{E}{2(1+\mu)}[C_{cc}^{00}D_{cc}^{00-1}E_{cc}^{11}+C_{cc}^{11}D_{cc}^{001}E_{cc}^{00}]+[k_{w0}+k_{wL}(-1)^{m+m'}]D_{cc}^{001}E_{cc}^{00}+R_1Kr(-1)^{n+n'}C_{cc}^{00}E_{cc}^{00}+R_1Kg(-1)^{n+n'}C_{cc}^{11}E_{cc}^{00}+R_1Kg(-1)^{n+n'}C_{cc}^{00}E_{cc}^{11}$$

$$\{\mathbf{K}_{7,8}\}_{f,e'}=\frac{E}{1-\mu^2}C_{cc}^{00}E_{cc}^{00}[D_{\zeta c}^{00-1}+D_{\zeta c}^{111}+\mu D_{\zeta c}^{010}+\mu D_{\zeta c}^{100}]+\frac{E}{2(1+\mu)}[C_{cc}^{00}D_{\zeta c}^{00-1}E_{cc}^{11}+C_{cc}^{11}D_{\zeta c}^{001}E_{cc}^{00}]$$

$$\{\mathbf{K}_{7,9}\}_{g,e'}=\frac{E}{1-\mu^2}C_{\zeta c}^{00}E_{cc}^{00}[D_{cc}^{00-1}+D_{cc}^{111}]+\frac{\mu E_2}{1-\mu^2}C_{\zeta c}^{00}E_{cc}^{00}[D_{cc}^{010}+D_{cc}^{100}]+\frac{E}{2(1+\mu)}[C_{\zeta c}^{00}D_{cc}^{00-1}E_{cc}^{11}+C_{\zeta c}^{11}D_{cc}^{001}E_{cc}^{00}]+R_1Kr(-1)^{n+n'}C_{\zeta c}^{00}E_{cc}^{00}+R_1Kg(-1)^{n+n'}C_{\zeta c}^{11}E_{cc}^{00}+R_1Kg(-1)^{n+n'}C_{\zeta c}^{00}E_{cc}^{11}$$

$$\{\mathbf{K}_{8,8}\}_{f,f'}=\frac{E}{1-\mu^2}C_{cc}^{00}E_{cc}^{00}[D_{\zeta\zeta}^{00-1}+D_{\zeta\zeta}^{111}+\mu D_{\zeta\zeta}^{010}+\mu D_{\zeta\zeta}^{100}]+\frac{E}{2(1+\mu)}[C_{cc}^{00}D_{\zeta\zeta}^{00-1}E_{cc}^{11}+C_{cc}^{11}D_{\zeta\zeta}^{001}E_{cc}^{00}]$$

$$\{\mathbf{K}_{8,9}\}_{g,f'}=\frac{E}{1-\mu^2}C_{\zeta c}^{00}E_{cc}^{00}[D_{c\zeta}^{00-1}+D_{c\zeta}^{111}+\mu D_{c\zeta}^{010}+\mu D_{c\zeta}^{100}]+\frac{E}{2(1+\mu)}[C_{\zeta c}^{00}D_{c\zeta}^{00-1}E_{cc}^{11}+C_{\zeta c}^{11}D_{c\zeta}^{001}E_{cc}^{00}]$$

$$\{\mathbf{K}_{9,9}\}_{g,g'}=\frac{E}{1-\mu^2}C_{\zeta\zeta}^{00}E_{cc}^{00}[D_{cc}^{00-1}+D_{cc}^{111}]+\frac{\mu E_2}{1-\mu^2}C_{\zeta\zeta}^{00}E_{cc}^{00}[D_{cc}^{010}+D_{cc}^{100}]+\frac{E}{2(1+\mu)}[C_{\zeta\zeta}^{00}D_{cc}^{00-1}E_{cc}^{11}+C_{\zeta\zeta}^{11}D_{cc}^{001}E_{cc}^{00}]+R_1Kr(-1)^{n+n'}C_{\zeta\zeta}^{00}E_{cc}^{00}$$

$$+R_1Kg(-1)^{n+n'}C^{11}_{\zeta\zeta}E^{00}_{cc}+R_1Kg(-1)^{n+n'}C^{00}_{\zeta\zeta}E^{11}_{cc}$$

and the elements in the stiffness matrix $\mathbf{M}$ are calculated according to the following formulations:

$$\{\mathbf{M}_{1,1}\}_{e,e'}=\rho C^{00}_{cc}D^{001}_{cc}E^{00}_{cc},\quad \{\mathbf{M}_{1,2}\}_{f,e'}=\rho C^{00}_{cc}D^{001}_{\zeta c}E^{00}_{cc},$$
$$\{\mathbf{M}_{1,3}\}_{g,e'}=\rho C^{00}_{\zeta c}D^{001}_{cc}E^{00}_{cc}$$

$$\{\mathbf{M}_{2,2}\}_{f,f'}=\rho C^{00}_{cc}D^{001}_{\zeta\zeta}E^{00}_{cc},\quad \{\mathbf{M}_{2,3}\}_{g,f'}=\rho C^{00}_{\zeta c}D^{001}_{c\zeta}E^{00}_{cc},$$
$$\{\mathbf{M}_{3,3}\}_{g,g'}=\rho C^{00}_{\zeta\zeta}D^{001}_{cc}E^{00}_{cc}$$

$$\mathbf{M}_{1,4},\mathbf{M}_{1,5},\ldots\mathbf{M}_{1,8},\mathbf{M}_{1,9}=\mathbf{0},\quad \mathbf{M}_{2,4},\mathbf{M}_{2,5},\ldots\mathbf{M}_{2,8},\mathbf{M}_{2,9}=\mathbf{0},$$
$$\mathbf{M}_{3,4},\mathbf{M}_{3,5},\ldots\mathbf{M}_{3,8},\mathbf{M}_{3,9}=\mathbf{0}$$

$$\{\mathbf{M}_{4,4}\}_{e,e'}=\rho C^{00}_{cc}D^{001}_{cc}E^{00}_{ss},\quad \{\mathbf{M}_{4,5}\}_{f,e'}=\rho C^{00}_{cc}D^{001}_{\zeta c}E^{00}_{ss},$$
$$\{\mathbf{M}_{4,6}\}_{g,e'}=\rho C^{00}_{\zeta c}D^{001}_{cc}E^{00}_{ss}$$

$$\{\mathbf{M}_{5,5}\}_{f,f'}=\rho C^{00}_{cc}D^{001}_{\zeta\zeta}E^{00}_{ss},\quad \{\mathbf{M}_{5,6}\}_{g,f'}=\rho C^{00}_{\zeta c}D^{001}_{c\zeta}E^{00}_{ss},$$
$$\{\mathbf{M}_{6,6}\}_{g,g'}=\rho C^{00}_{\zeta\zeta}D^{001}_{cc}E^{00}_{ss}$$

$$\mathbf{M}_{4,7},\mathbf{M}_{4,8},\mathbf{M}_{4,9},\mathbf{M}_{5,7},\mathbf{M}_{5,8},\mathbf{M}_{5,9},\mathbf{M}_{6,7},\mathbf{M}_{6,8},\mathbf{M}_{6,9}=\mathbf{0}$$

$$\{\mathbf{M}_{7,7}\}_{e,e'}=\rho C^{00}_{cc}D^{001}_{cc}E^{00}_{cc},\quad \{\mathbf{M}_{7,8}\}_{f,e'}=\rho C^{00}_{cc}D^{001}_{\zeta c}E^{00}_{cc},$$
$$\{\mathbf{M}_{7,9}\}_{g,e'}=\rho C^{00}_{\zeta c}D^{001}_{cc}E^{00}_{cc}$$

$$\{\mathbf{M}_{8,8}\}_{f,f'}=\rho C^{00}_{cc}D^{001}_{\zeta\zeta}E^{00}_{cc},\quad \{\mathbf{M}_{8,9}\}_{g,f'}=\rho C^{00}_{\zeta c}D^{001}_{c\zeta}E^{00}_{cc},$$
$$\{\mathbf{M}_{9,9}\}_{g,g'}=\rho C^{00}_{\zeta\zeta}D^{001}_{cc}E^{00}_{cc}$$

where

$$C^{ab}_{cc}=\int_0^L\frac{d^a\ \cos\ \lambda_m x}{dx^a}\frac{d^b\ \cos\ \lambda_{m'}x}{dx^b}dx,$$
$$C^{ab}_{\zeta c}=\int_0^L\frac{d^a\zeta_l(x)}{dx^a}\frac{d^b\ \cos\ \lambda_{m'}x}{dx^b}dx$$

$$C^{ab}_{c\zeta}=\int_0^L\frac{d^a\ \cos\ \lambda_m x}{dx^a}\frac{d^b\zeta_{l'}(x)}{dx^b}dx,$$
$$C^{ab}_{\zeta\zeta}=\int_0^L\frac{d^a\zeta_l(x)}{dx^a}\frac{d^b\zeta_{l'}(x)}{dx^b}dx$$

$$D^{abc}_{cc}=\int_0^h\frac{d^a\ \cos\ \lambda_q\bar{r}}{d\bar{r}^a}\frac{d^b\ \cos\ \lambda_{q'}\bar{r}}{d\bar{r}^b}(\bar{r}+R_0)^c d\bar{r},$$
$$D^{abc}_{\zeta c}=\int_0^h\frac{d^a\zeta_l(\bar{r})}{d\bar{r}^a}\frac{d^b\ \cos\ \lambda_{q'}\bar{r}}{d\bar{r}^b}(\bar{r}+R_0)^c d\bar{r}$$

$$D^{abc}_{c\zeta}=\int_0^h\frac{d^a\ \cos\ \lambda\bar{r}}{d\bar{r}^a}\frac{d^b\zeta_{l'}(\bar{r})}{d\bar{r}^b}(\bar{r}+R_0)^c d\bar{r},$$
$$D^{abc}_{\zeta\zeta}=\int_0^h\frac{d^a\zeta_l(\bar{r})}{d\bar{r}^a}\frac{d^b\zeta_{l'}(r)}{d\bar{r}^b}(\bar{r}+R_0)^c d\bar{r}$$

$$E^{ab}_{cc}=\int_0^{2\pi}\frac{d^a\ \cos(n\theta)}{d\theta^a}\frac{d^b\ \cos(n\theta)}{d\theta^b}d\theta,$$
$$E^{ab}_{ss}=\int_0^{2\pi}\frac{d^a\ \sin(n\theta)}{d\theta^a}\frac{d^b\ \sin(n\theta)}{d\theta^b}d\theta$$

$$E^{ab}_{cs}=\int_0^{2\pi}\frac{d^a\ \cos(n\theta)}{d\theta^a}\frac{d^b\ \sin(n\theta)}{d\theta^b}d\theta,$$
$$E^{ab}_{sc}=\int_0^{2\pi}\frac{d^a\ \sin(n\theta)}{d\theta^a}\frac{d^b\ \cos(n\theta)}{d\theta^b}d\theta$$

where $d^af(\xi)/d\xi^a$ represents the a-order derivative of function $f(\xi)$ with respect to ξ (ξ=x,θ or $\bar{r}$).

References

[1] Arnold RN, Warburton GB. Flexural vibrations of the walls of thin cylindrical shells having freely supported ends. Proc Roy Soc 1949;197(A):238–56.
[2] Qu Y, Wu S, Chen Y, Hua H. Vibration analysis of ring-stiffened conical–cylindrical–spherical shells based on a modified variational approach. Int J Mech Sci 2013;69:78–84.
[3] Forsberg K. Influence of boundary conditions on the modal characteristics of thin cylindrical shells. AIAA J 1964;2:2150–7.
[4] Warburton GB. Vibration of thin cylindrical shells. Int J Mech Sci 1965;7:399–407.
[5] Qu Y, Chen Y, Long X, Hua H, Meng G. Free and forced vibration analysis of uniform and stepped circular cylindrical shells using a domain decomposition method. Appl Acoust 2013;74:425–39.
[6] Bert CW, Malik M. Free vibration analysis of thin cylindrical shells by the differential quadrature method. J Pres Vess Tech 1996;118:1–12.
[8] Lam KY, Loy CT. Effects of boundary conditions on frequencies of a multi-layered cylindrical shell. J Sound Vib 1995;188(3):363–84.
[7] Loy CT, Lam KY. Vibration of cylindrical shells with ring support. Int J Mech Sci 1997;39(4):455–71.
[9] Zhang XM, Liu GR, Lam KY. Vibration analysis of thin cylindrical shells using wave propagation approach. J Sound Vib 2001;239:397–403.
[10] Weingarten VI. Free vibration of thin cylindrical shells. AIAA J 1964;2:717–22.
[11] Chen Y, Jin G, Liu Z. Free vibration analysis of circular cylindrical shell with non-uniform elastic boundary constraints. Int J Mech Sci 2013;74:120–32.
[12] Hajianmaleki M, Qatu MS. Transverse vibration analysis of generally laminated two-segment composite shafts with a lumped mass using generalized differential quadrature. J Vib Control 2013;19(13):2013–21.
[13] Asadi E, Wang W, Qatu MS. Static and vibration analyses of thick deep laminated cylindrical shells using 3D and various shear deformation theories. Compos Struct 2012;94(2):494–500.
[14] Jin G, Ye T, Ma X, Chen Y, Su Z, Xie X. A unified approach for the vibration analysis of moderately thick composite laminated cylindrical shells with arbitrary boundary conditions. Int J Mech Sci 2013;75:357–76.
[15] Jin G, Ye T, Jia X, Gao S. A general Fourier solution for the vibration analysis of composite laminated structure elements of revolution with general elastic restraints. Compos Struct 2014;109:150–68.
[16] Bhimaraddi A. A higher order theory for free vibration analysis of circular cylindrical shells. Int J Solids Struct 1984;20(7):623–30.
[17] Reddy JN. On refined computational models of composite laminates. Int J Numer Methods Eng 1989;27(2):361–82.
[18] Loy CT, Lam KY. Vibration of thick cylindrical shells on the basis of three-dimensional theory of elasticity. J Sound Vib 1999;226(4):719–37.
[19] Zhou D, Cheung YK, Lo SH, Au FTK. 3D vibration analysis of solid and hollow circular cylinders via Chebyshev–Ritz method. Comput Methods Appl Mech Eng 2003;192:1575–89.
[20] Mofakhami MR, Toudeshky HH, Hashemi SH. Finite cylinder vibrations with different end boundary conditions. J Sound Vib 2006;297:293–314.
[21] Hutchinson JR. Vibrations of solid cylinders. J Appl Mech 1980;47:901–7.
[22] Leissa AW, Kang JH. Three-dimensional vibration analysis of thick shells of revolution. J Eng Mech 1999;125:1365–71.
[23] Khalili SMR, Davar A, Fard KM. Free vibration analysis of homogeneous isotropic circular cylindrical shells based on a new three-dimensional refined higher-order theory. Int J Mech Sci 2012;56:1–25.
[24] Soldatos KP, Hadjigeorgiou VP. Three-dimensional solution of the free vibration problem of homogeneous isotropic cylindrical shells and panels. J Sound Vib 1990;137(3):369–84.
[25] Chen WQ, Bian ZG, Ding HJ. Three-dimensional vibration analysis of fluid-filled orthotropic FGM cylindrical shells. Int J Mech Sci 2004;46(1):159–71.
[26] Kant T, Kumar S, Singh UP. Shell dynamics with 3D degenerate FES. Comput Struct 1994;50(1):135–46.
[27] Liew KM, Hung KC. Three-dimensional vibratory characteristics of solid cylinders and some remarks on simplified beam theories. Int J Solids Struct 1995;32(23):3499–513.
[28] Mizusawa T, Kato T. Application of the spline prism method to analyse vibration of thick circular cylindrical panels. Int J Solids Struct 1996;33(7):967–76.
[29] So J, Leissa AW. Free vibrations of thick hollow circular cylinders from three-dimensional analysis. J Vib Acoust 1997;119:89–95.
[30] Kang JH, Leissa AW. Three-dimensional vibrations of hollow cones and cylinders with linear thickness variation. J Acoust Soc Am 1999;106(2):748–55.
[31] Armenakas AE, Gazis DC, Herrmann G. Free vibrations of circular cylindrical shells. Oxford: Pergamon Press; 1969.
[32] Liew KM, Hung KC. Three-dimensional vibratory characteristics of solid cylinders and some remarks on simplified beam theories. Int J Solids Struct 1995;32(23):3499–513.
[33] Leissa AW, Qatu MS. Vibrations of continuous systems. New York: McGraw Hills; 2011.
[34] Qatu MS. Recent research advances in the dynamic behavior of shells: 1989-2000, part 2: homogeneous shells. Appl Mech Rev 2002;55(5):415–34.
[35] Soldatos KP. Review of three-dimensional dynamic analyses of circular cylinders and cylindrical shells. Appl Mech Rev 1994;47(10):501–16.

[36] Malekzadeh P, Farid M, Zahedinejad P, Karami G. Three-dimensional free vibration analysis of thick cylindrical shells resting on two-parameter elastic supports. J Sound Vib 2008;313:655–75.
[37] Tj HG, Mikami T, Kanie S, Sato M. Free vibration characteristics of cylindrical shells partially buried in elastic foundations. J Sound Vib 2006;290:785–93.
[38] Paliwal DN, Pandey RK, Nath T. Free vibrations of circular cylindrical shell on Winkler and Pasternak foundations. J Pres Vess Pip 1996;69:79–89.
[39] Shah AG, Mahmood T, Naeem MN, Arshad SH. Vibration characteristics of fluid-filled cylindrical shells based on elastic foundations. Acta Mech 2011;216:17–28.
[40] Liu JX, Li TY, Liu TG, Yan J. Vibration characteristic analysis of buried pipes using the wave propagation approach. Appl Acoust 2005;66:353–64.
[41] Li WL. Free vibrations of beams with general boundary conditions. J Sound Vib 2000;237(4):709–25.
[42] Li WL. Comparison of Fourier sine and cosine series expansions for beams with arbitrary boundary conditions. J Sound Vib 2002;255(1):185–94.
[43] Zhang X, Li WL. Vibrations of rectangular plates with arbitrary non-uniform elastic edge restraints. J Sound Vib 2009;326:221–34.
[44] Jin G, Su Z, Shi S, Ye T, Gao S. Three-dimensional exact solution for the free vibration of arbitrarily thick functionally graded rectangular plates with general boundary conditions. Compos Struct 2014;108:565–77.